

Article

Quantification of the Microwave Effect in the Synthesis of 5-Hydroxymethylfurfural over Sulfonated MIL-101(Cr)

Noor Aljammal^{1,2}, Jeroen Lauwaert^{3,*}, Bert Biesemans¹, Francis Verpoort^{4,5},
Philippe M. Heynderickx^{2,6} and Joris W. Thybaut^{1,*}

- ¹ Laboratory for Chemical Technology (LCT), Department of Materials, Textiles, and Chemical Engineering, Ghent University, Technologiepark 125, B-9052 Ghent, Belgium
- ² Department of Green Chemistry and Technology, Faculty of Bioscience Engineering, Ghent University, Coupure Links 653, B-9000 Ghent, Belgium
- ³ Industrial Catalysis and Adsorption Technology (INCAT), Department of Materials, Textiles, and Chemical Engineering, Ghent University, Valentin Vaerwyckweg 1, B-9000 Ghent, Belgium
- ⁴ Laboratory of Organometallics, Catalysis and Ordered Materials, State Key Laboratory of Advanced Technology for Materials Synthesis and Processing, Wuhan University of Technology, 122 Luoshi Road, Wuhan 430070, China
- ⁵ Research School of Chemistry & Applied Biomedical Sciences, National Research Tomsk Polytechnic University, Lenin Avenue 30, 634050 Tomsk, Russia
- ⁶ Center for Environmental and Energy Research (CEER)—Engineering of Materials via Catalysis and Characterization, Ghent University Global Campus, 119-5 Songdomunhwa-ro, Yeonsu-gu, Incheon 406-840, Republic of Korea
- * Correspondence: jeroen.lauwaert@ugent.be (J.L.); joris.thybaut@ugent.be (J.W.T.)

Abstract: The potential benefits of microwave irradiation for fructose dehydration into 5-hydroxymethylfurfural (5-HMF) have been quantified over a sulfonated metal–organic framework (MOF), MIL 101(Cr)-SO₃H. The effects of temperature (140–170 °C), batch time (5–300 min), and catalyst-to-substrate ratio (0.1–0.01 g/g) were systematically mapped. After 10 min of microwave (MW) irradiation at 140 °C in a DMSO–acetone reaction medium, practically complete fructose conversion was obtained with a 70% yield of 5-HMF. Without MW, i.e., using conventional heating (CH) at the same conditions, the fructose conversion was limited to 13% without any 5-HMF yield. Rather, 90 min of CH was required to reach a similarly high conversion and yield. The profound impact of moving from CH towards MW conditions on the reaction kinetics, also denoted as the microwave effect, has been quantified through kinetic modeling via a change in the Gibbs free energy of the transition state. The modeling results revealed an eight-fold rate coefficient enhancement for fructose dehydration owing to MW irradiation, while the temperature dependence of the various reaction steps almost completely disappeared in the investigated range of operating conditions.

Keywords: sugar; 5-HMF; kinetics; microwave; MOFs



Citation: Aljammal, N.; Lauwaert, J.; Biesemans, B.; Verpoort, F.; Heynderickx, P.M.; Thybaut, J.W. Quantification of the Microwave Effect in the Synthesis of 5-Hydroxymethylfurfural over Sulfonated MIL-101(Cr). *Catalysts* **2023**, *13*, 622. <https://doi.org/10.3390/catal13030622>

Academic Editors: Hugo de Lasa and Mohammad Mozahar Hossain

Received: 13 February 2023

Revised: 12 March 2023

Accepted: 16 March 2023

Published: 20 March 2023



Copyright: © 2023 by the authors. Licensee MDPI, Basel, Switzerland. This article is an open access article distributed under the terms and conditions of the Creative Commons Attribution (CC BY) license (<https://creativecommons.org/licenses/by/4.0/>).

1. Introduction

Currently, there is a rising need for sustainable production of platform chemicals and renewable fuels, which can be used together with fossil fuels or even replace them entirely. Biorefineries emerge as alternatives to petroleum-based ones, as biomass is an abundant, relatively cheap, renewable feedstock [1]. Raw biomass usually has an unfavorable size distribution, low bulk density, and, hence, low volumetric energy density. Therefore, several pre-treatments (e.g., mechanical and chemical) are essential for enhancing the properties of the feedstock [2]. For example, degradation of cellulose and hemicellulose results in the formation of sugars, which can be used as versatile starting materials for producing a variety of value-added products, such as 5-hydroxymethylfurfural (5-HMF) which is classified among the top 10 most valuable biomass-based chemicals [3]. 5-HMF can be obtained from fructose via triple dehydration over Brønsted acid sites [4–6]. Another possibility is the

conversion of glucose, but this is more challenging compared to fructose owing to the additionally required isomerization step. Once formed, HMF can be converted to secondary platform chemicals (SPCs) [7] such as C9-C15 alkanes [8,9], 2,5-furandicarboxylic acid (FDCA) [5,10–12], ethyl levulinate (EL) [13,14], and 5-ethoxymethylfurfural (5-EMF) [15]. Through hydrolysis, HMF can be converted into γ -valerolactone (GVL) [13], which has long been known as a potential green fuel—‘a liquid with high-energy density’, fuel additive and solvent [16–24]. The intermediate product 5-HMF can be decomposed into levulinic acid or formic acid [25,26], polymerized to humic acids, and converted to dialdehyde in the presence of oxidative species [27]. The selectivity towards each type of product that may result from any reaction varies according to various factors including the type of catalyst, the solvent used, and the operating temperature, which can be manipulated to steer the reaction to the desired pathway [28,29]. Accordingly, research on developing novel strategies and the optimization of existing strategies to produce this five-membered ring compound using homogenous and heterogeneous catalysis is on the rise [30]. The literature offers many examples of 5-HMF production routes comprising thermally induced dehydration of fructose, typically in dimethyl sulfoxide (DMSO) over homogeneous acid catalysts (HCl, H₂SO₄, H₃PO₄, oxalic or levulinic acid) [31–34]. However, despite the high 5-HMF yields (40 to 60%) obtained via homogenous catalysis, in such processes, the catalysts are difficult to recover and reuse, require energy-intensive separation, and are frequently responsible for equipment corrosion [35,36]. Moreover, low product selectivity and stability are contemporary challenges impeding the broad implementation and commercialization of many catalytic biomass conversion processes [37]. Hence, the endeavor to develop sustainable processes for the production of added-value chemicals and fuels triggered researchers to overcome these challenges via novel heterogeneous catalysts and non-conventional heating technologies. Non-conventional heating technologies in particular have been explored to improve biomass conversion in relation to conventional heating (CH) [38–41]. Among these techniques, the use of microwave (MW) irradiation to drive chemical reactions seems most widely appreciated and utilized by organic chemists, both in academia and industries such as food processing, textiles, papermaking, and ceramics [42–45]. Since discovery of the beneficial effects of MW irradiation on biomass valorization, its number of applications towards catalysis for organic synthesis has increased dramatically [43,46–49]. Early studies reported that MW irradiation could increase reaction rates by a factor of between 5 and 1000 compared to CH [41]. Hence, the most significant benefit of MW irradiation in chemical synthesis is the substantial reduction in required reaction time. Moreover, MW irradiation has been claimed to ensure fast and selective heating, lower energy consumption, and controllable processing [42,46]. Moreover, under MW irradiation, the production of biomass-based platform chemicals can already occur at distinctly lower temperatures compared to CH. Consequently, fewer functional groups are lost during the reaction, and the obtained molecules thus retain a high degree of functionality compared to the ones obtained after CH [46].

The heat transfer under microwave irradiation depends on several factors, such as the size and the properties of the targeted material. In general, MW dissipation is attributed to (i) dielectric loss heating and (ii) magnetic loss heating [50]. The latter refers to the energy dissipated when the alternate magnetic field acts on a ferro- or ferrimagnetic material. Compared to magnetic loss materials, more attention is paid to the investigation of dielectric loss materials [51]. Dielectric loss heating is based on the dielectric properties of the material, such as the permittivity or the dielectric constant (ϵ) and the dielectric loss (ϵ''). While the former represents a measure of the capacity of a dielectric material to store electric energy, that is, to polarize under the varying electrical field [52], the latter quantifies the relaxation time (lag) between the electric field and the polarization movement of molecules, which causes energy dissipation as heat. Dielectric loss (ϵ'') can be parameterized in terms of tangent delta (δ) or loss tangent, which is defined as the ratio of ϵ'' to ϵ . This ratio represents the dissipation factor of the sample [53], which indicates the ability of a material to absorb electric charges and how efficiently MW energy is converted into thermal energy.

For example, depending on the tangent delta (δ), materials are classified as exhibiting high ($\tan \delta > 0.5$), medium ($0.5 \geq \tan \delta \geq 0.1$), or low ($\tan \delta < 0.1$) microwave absorption [52]. Metal-based materials, such as metal-containing catalysts, metal oxide/sulfide/phosphate, and magnetic metals, alloys, etc., are considered microwave-absorbing materials due to their high $\tan \delta$ values.

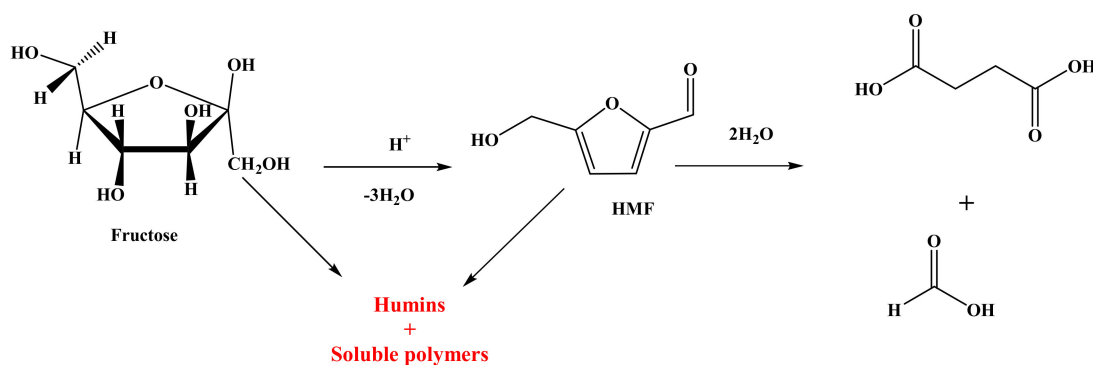
In this context, the application of metal-containing solid catalysts in microwave-assisted organic synthesis (MAOS) was introduced by Varma [54]. Due to the excellent microwave-absorbing capacity of metal catalysts, the MW irradiation energy is rapidly and effectively transformed into heat throughout the system. Much attention has also been given in the literature to the actual origin of the rate enhancement under MW heating, such as determining whether it is a purely thermal effect [55–57] or, as some researchers suggest, a non-thermal effect [44,58–60] in which the microwave energy itself directly couples to energy modes within the molecule or lattice. Disagreement exists as to whether, in case the microwave effect is not purely thermal, it should be referred to as “non-thermal”, “non-purely thermal”, or simply a “specific effect”. Indeed, the thought of specific microwave effects has been floated by many researchers [42,60–63]. The occurrence of such a microwave-specific effect has significant implications for reaction chemistry. It proposes that MW effects on solid surfaces might deliver energetic and mechanistic advantages to catalytic reactions [60,64]. In this respect, microwave-irradiated catalyst particles have been considered an indirect heat source [65]. In addition, upon MW irradiation, electron pairs of the catalyst can be excited directly (electron–hole), generating free radicals at its surface [66]. This combined effect can significantly improve catalytic activity. As a result, such a system is often referred to as an MW-enhanced catalytic process. An excellent review by Török and coworkers covers the development of MW instrumentation, theories, and applications, highlighting MW-assisted reactions with transition metal-containing catalysts [67].

Among heterogeneous acid catalysts, metal–organic frameworks (MOFs) recently gained attention for biomass conversion [68–72]. MOFs are a class of nanoporous crystalline materials that consist of regular clusters of positively charged metal ions surrounded by organic linker molecules. The remarkable control, scalability, and modifiable characteristics of the reticular chemistry inherent to MOFs result in materials that are almost unlimited in their functional potential [73–80]. Since the discovery of the remarkable catalytic capabilities of MOFs for biomass conversion, a lot of work has been aimed at investigating the dehydration of various hexoses into hydroxymethylfurfural (5-HMF) over a wide range of pristine and modified MOFs. The acidic properties of some MOFs can, indeed, be further enhanced by adding functional groups such as nitro, sulfate, or phosphate to their structure to tune Brønsted and Lewis acid sites [68,69,81–84]. The high activity and selectivity of sulfonated MOFs make $-\text{SO}_3\text{H}$ the ‘functional group’ of choice for these reactions [65,68,84–86].

Merging microwave-responsive catalysts such as functionalized MOFs (polar absorber hybrid materials) with contemporary MW technology could contribute positively to sustainable biomass conversion towards useful renewable products. One type of MOF exhibiting high thermal and chemical stability, MIL-101(Cr), has been used as a solid catalyst for MW-assisted biomass conversion reactions [82,87,88]. The acronym “MIL” stands for “Material from Institut Lavoisier”, while the number “101” refers to the fact that it was the first MOF developed at the Institut Lavoisier. The high catalytic activity of this MOF is attributed to the chromium ions, Cr (III), which are highly active Lewis acid sites. These sites are beneficial for biomass transformation as they can act as binding sites for solvent molecules or fructose to catalyze the formation of 5-HMF [9]. However, it should be noted that, when used as a homogenous catalyst (i.e., CrCl_2), the chromium ions entail many environmental and health risks [89,90]. However, even if the use of the metal (Cr) is not eliminated, embedding them in heterogeneous structures (as is the case in MIL-101(Cr)) significantly reduces these risks [91]. Recently, there has also been a drive to investigate the potential replacement of Cr with nontoxic metals such as Sc and Fe to prepare even more environmentally benign catalysts. These MIL-101 analogues have also been assessed for

5-HMF production, but their performance does not meet that of MIL-101(Cr), especially in terms of stability [72]. Therefore, several studies selected the latter for further investigations on catalyst performance for biomass conversion [82,87,88].

Robust functionalized MIL-101(Cr) with a Brønsted acid functional group, e.g., sulfonic MIL-101(Cr)-SO₃H, made it superior to conventional solid acid catalysts such as acidic oxides, acid resins, phosphates, and zeolite-based catalysts [1,92,93]. MIL-101(Cr)-SO₃H has shown good catalytic performance in converting fructose into 5-HMF [82,84,86]. Moreover, the sulfonated MIL-101 (Cr) has two excellent microwave-absorbing sites, i.e., the chromium and the sulfonic acid group [54,94]. Since MIL-101(Cr)-SO₃H possesses strong acid sites, fructose dehydration is likely to occur through an E1 elimination reaction [84,95]. As depicted in Scheme 1, fructose is dehydrated to 5-HMF, which further converts into levulinic acid (LA) and formic acid (FA) in equimolar quantities [96]. As the main undesirable side reaction, fructose and/or 5-HMF can also react to form soluble and insoluble humins [97–99]. In addition, cross-condensations between 5-HMF and sugars have also been reported to form humins [82,100]. Understanding and controlling these side reactions is a major challenge [25,96]. MIL-101(Cr)-SO₃H does not only enhance the dehydration rate, but also accelerates the formation of undesired products such as humins. Hence, further investigation of the exact catalytic performance of MIL-101(Cr)-SO₃H for sugar conversion is still needed to better understand its application potential [84].



Scheme 1. Reaction scheme of fructose dehydration to 5-HMF and parallel reactions.

As previously mentioned, the effects of MW irradiation on organic synthesis remain a subject of intense debate, and experimental research is currently underway to clarify these effects. Therefore, it is imperative to elucidate these effects through kinetic modeling. This work aims to provide novel insights into the MW effect via kinetic modeling, enabling a deeper understanding of the fundamental mechanisms and principles governing reaction kinetics and thermodynamics under microwave conditions. Quantification of the microwave effect in terms of changes in enthalpy and entropy is critical in optimizing reaction conditions and improving reaction performance with the aim of increasing reaction rate and selectivity. Furthermore, an extensive understanding of the thermodynamics of the microwave effect can significantly contribute to the development of innovative microwave-assisted synthetic methodologies and the advancement of novel microwave-assisted reactions.

In this work, we evaluated MIL 101(Cr) SO₃H as a microwave-responsive catalyst for fructose dehydration to 5-HMF within the temperature range of 140–170 °C. First, we experimentally assessed the improvement in catalyst performance by MW irradiation compared to CH, aiming to elucidate the effects of temperature, solvent, catalyst structure, and MW irradiation. Subsequently, we used the obtained dataset to develop a kinetic model capturing the effects of reaction conditions. Within the model, the MW effect is quantified in terms of a change in Gibbs free energy in the transition state. To the best of our knowledge, this is the first model capable of describing a reaction performed under both CH and MW irradiation.

2. Results and Discussion

2.1. Preliminary Screening of the Dehydration Conditions

Preliminary tests for fructose dehydration into 5-HMF allowed reaction performance in response to the MW power mode to be evaluated via the sulfonic acid groups ($-\text{SO}_3\text{H}$) on the catalyst. Additionally, the solvent composition effect on reaction performance was evaluated, as well as that of the catalyst mass.

2.1.1. Sulfonic Acid Group Loading Effect

The effect of sulfonic acid group loading on reaction performance was first investigated. A meager 5-HMF yield was obtained for MIL-101(Cr) without any sulfonic groups, which is not surprising since it does not possess any Brønsted acidity. The 5-HMF yield increased almost linearly with $-\text{SO}_3\text{H}$ loading on the other investigated samples (see Table 1). It can also be observed that with higher sulfur content, higher 5-HMF selectivity can be obtained. However, the possibility of 5-HMF reacting with two water molecules in a rehydration reaction will increase, forming levulinic acid and formic acid [82]. This finding logically agrees with the increasing number of Brønsted acid sites grafted on the catalyst [101]. Apart from that, the excellent microwave absorption ability of the sulfonic groups should not be forgotten. Previous research proved that polar absorber hybrid materials (e.g., materials containing $-\text{SO}_3\text{H}$) significantly impact enhancement of the dielectric and microwave-absorbing properties of the modified material [65,102,103]. Those findings can help prepare promising microwave-absorbing materials at 2–18 GHz frequency for absorbing applications [102].

Table 1. Effect of different $-\text{SO}_3\text{H}$ loadings on MIL-101(Cr) in terms of 5-HMF yield. Reaction conditions: MW using the standard power mode, 100 mg fructose (0.56 mmol), 3 mL solvent, DMSO/acetone 70/30, performed over 10 mg catalyst for 5 min at 160 °C. The total sulfur content of MIL-101- SO_3H samples was determined by elemental analysis (C, H, N, S) using a Flash EA1112 instrument.

Catalyst Type	S Content [mmol g ⁻¹]	Fructose Conv. [%]	Yield [%]			Selectivity [%]		
			5-HMF	FA	LA	5-HMF	FA	LA
MIL-101(Cr)	-	99	9	0	0	9	0	0
MIL-101(Cr)- SO_3H (1)	0.23	98	38	0	1	39	0	0
MIL-101(Cr)- SO_3H (2)	0.56	99	54	2	1	55	2	0
MIL-101(Cr)- SO_3H (3)	0.91	98	61	14	13	62	14	13

The 5-HMF yield with MIL-101(Cr)- SO_3H (3) was seven-fold higher than that of the parent MOF without sulfonic acid groups (MIL-101(Cr)). The detailed mechanism showing the importance of $-\text{SO}_3\text{H}$ acid groups in the elimination reaction can be found in Supplementary Materials S4. In our previous work, the catalyst's stability was proven for at least three cycles [1].

Concerning the performance enhancement under MW conditions, previous research demonstrated that the frequent alignment of polar sulfonic acid groups with the alternating electromagnetic field forces the strong vibration of polar groups and friction with neighboring molecules, thus increasing the probability of molecular collision between reactants and catalysts [104–106]. In fructose dehydration over MIL-101(Cr)- SO_3H , the polar sulfonic acid group is envisioned to rotate quickly in the MW field [101,107]. This then facilitates the reactant transformation from the ground state to the transition state, which increases reactivity towards 5-HMF formation [41]. This can be attributed to the fact that MW irradiation can enhance electron transfer from the MOF's cluster to the attached sulfonic groups, resulting in the enhanced acidity and polarity of sulfonic groups [101]. As a result of these rapid motions, heating also occurs faster, which is another factor enhancing catalytic performance [101]. Additionally, CH_2OH groups on the fructose molecules and alcohol functions in 5-HMF respond to MW irradiation and contribute to heating of the reacting system.

2.1.2. Solvent Effect on Fructose Dehydration Using MW Heating

Fructose dehydration was performed in mixtures of DMSO and acetone with different molar ratios. This system was selected based on previous extensive laboratory screening tests of fructose dehydration over several MOFs [82]. The efficiency of various solvents in catalytic fructose dehydration was investigated, including water, ethanol, high-boiling-point polar aprotic organic solvents such as DMSO, and biphasic systems. DMSO was found to be the most efficient due to its polarity, which promotes reaction steps that lead to a high yield of HMF. However, DMSO's boiling point limits its application. Acetone/DMSO mixtures were discovered to effectively improve selectivity towards 5-HMF formation [82]. Moreover, both DMSO and acetone are dipolar aprotic solvents that have a tendency to associate through dipole–dipole interactions. Acetone is employed to stabilize 5-HMF and prevent further reaction to LA and FA [101]. At the same time, DMSO is required to ensure good fructose solubility in the solvent [108]. DMSO is a high MW irradiation absorber with significant dielectric losses. It thus heats very quickly within the microwave chamber (see Table 2). DMSO alignment to the applied electric field is presented in Supplementary Materials S3.

Table 2. Dielectric constant (ϵ), $\tan \delta$, and dielectric loss (ϵ'') for DMSO and acetone (measured at room temperature and 2450 MHz) [53].

Solvent (Tb °C)	Dielectric Constant (ϵ)	Dielectric Loss (ϵ'')	Tangent Delta (δ)
DMSO (189)	45.0	37.1	0.825
Acetone (56)	20.7	1.1	0.054

DMSO has been demonstrated to dissociate into $[\text{CH}_2\text{O}]$ and $[\text{CH}_3\text{SH}]$ at high temperatures (i.e., >180 °C), which could then take up a catalyzing role [109]. Therefore, experiments were performed to ensure the absence of such a homogeneous catalytic effect from the solvent within our selected range of reaction conditions (see Table 3). The result proves that DMSO does not decompose at temperatures below 190 °C within the investigated reaction time. Thus, the homogeneous species were not formed at the targeted reaction temperature range [110,111]. Therefore, the assumption that the solvent does not impact reaction rates is justified. Moreover, it is also understood from the full fructose conversion in the absence of a catalyst that the catalyst's role is to steer reaction selectivity towards 5-HMF production, i.e., to not simply activate the fructose but to also enhance the desired reaction compared to others in the reaction scheme.

Table 3. Non-catalytic fructose dehydration into 5-HMF. Reaction conditions: MW via the standard power mode, 100 mg fructose (0.56 mmol), 3 mL solvent, DMSO/acetone 70/30.

Temperature (°C)	Type of Heating	Time [min]	Fructose Conv. [%]	Yield [%]		
				5-HMF	FA	LA
150	MW	5	>99	0	0	0
160	MW	5	>99	0	0	0
170	MW	5	>99	trace	trace	trace
160	CH	60	>99	0	0	0

Catalytic reactions showed that 5-HMF selectivity increased with DMSO content in the solvent (see Table 4). A maximum 5-HMF selectivity of 61% was observed after 5 min for the 70:30 DMSO/acetone mixture at MW conditions. Moreover, fructose has been shown to rearrange to the furanoid form, which is more selectively converted into 5-HMF, consequently avoiding undesirable side reactions [108]. Thus, the optimal DMSO/acetone ratio of 70:30 was selected for further experimental investigation.

Table 4. Solvent effect of 5-HMF production from fructose over MIL-101(Cr)-SO₃H(3) ([H⁺] 0.009 mmol). Reaction conditions: MW via the standard power mode, 100 mg fructose (0.56 mmol), 3 mL solvent, performed over 10 mg catalyst at 160 °C.

Catalyst Wt. [mg]	Time [min]	Solvent	Fructose Conv. [%]	Yield [%]		
				5-HMF	FA	LA
30	50	DMSO	98	36	22	39
30	50	DMSO/Acetone 70:30	98	48	17	25
10	5	DMSO/Acetone 70:30	>99	61	14	13
10	5	DMSO/Acetone 60:40	>99	11	trace	trace
10	5	DMSO/Acetone 50:50	>99	8	trace	trace
10	5	DMSO/Acetone 30:70	>99	0	0	0

It should be noted that the amount of catalyst used can also affect the distribution of products, with higher selectivity to 5-HMF observed when a lower amount of catalyst (10 mg) is employed. This is because catalyst loading determines the number of available acidic sites that facilitate both the formation of the desired 5-HMF and the polymerization of 5-HMF and fructose into undesirable byproducts [112]. Therefore, an optimized catalyst loading of 10 mg was used in this study.

2.1.3. Batch Time Evolution

As ‘batch time’, defined as the product of catalyst mass and reaction time, is one of the major factors determining the extent of a chemical reaction [113], it was screened next. Fructose conversion and product yield as a function of batch time is given in Figure 1. Increasing batch time from 3 to 36 g·s significantly improves 5-HMF yield from 60% to 89%, respectively. However, further increasing batch time resulted in a decrease in 5-HMF yield, while the yield of LA and FA further increased. Furthermore, an unavoidable phenomenon was observed at longer reaction times; the mixture gradually changed from an orange to a dark brown dense liquid due to humin formation [114]. This finding was most pronounced at CH conditions and is attributed to an unfavorable caramelization reaction during sugar heating in the presence of the acid catalyst, which is a combination of aldose–ketose isomerization, dehydration, and anomeric–cyclic equilibrium [115].

The most considerable benefit of MW irradiation in chemical synthesis is the significant reduction in total reaction time (see Table 5). The effect of MW irradiation on chemical reactions is generally evaluated by comparing the time needed to obtain the maximum yield of final products with respect to CH. In comparing the two operating modes, as displayed in Table 5, it is clear that the MW-driven reaction is faster than the equivalent CH process. At 160 °C, the batch time in the MW reactor was reduced to 3 g·s, while at CH conditions, a more than 10-fold higher batch time was needed to reach a similar 5-HMF yield. More experimental data for product evolution with batch time are available in Supplementary Materials S5.

Table 5. Comparison between MW and CH for fructose dehydration. Reaction conditions: 100 mg fructose (0.56 mmol), 10 mg MIL-101(Cr)-SO₃H(3) ([H⁺] 0.009 mmol), 3 mL DMSO/acetone (70:30), performed at a temperature of 160 °C.

Method of Heating	Temperature [°C]	Batch Time [g·s]	Catalyst [mg]	Fructose Conv. [%]	5-HMF Yield [%]
MW	160	3	10	95	61
CH	160	36	10	>99	60

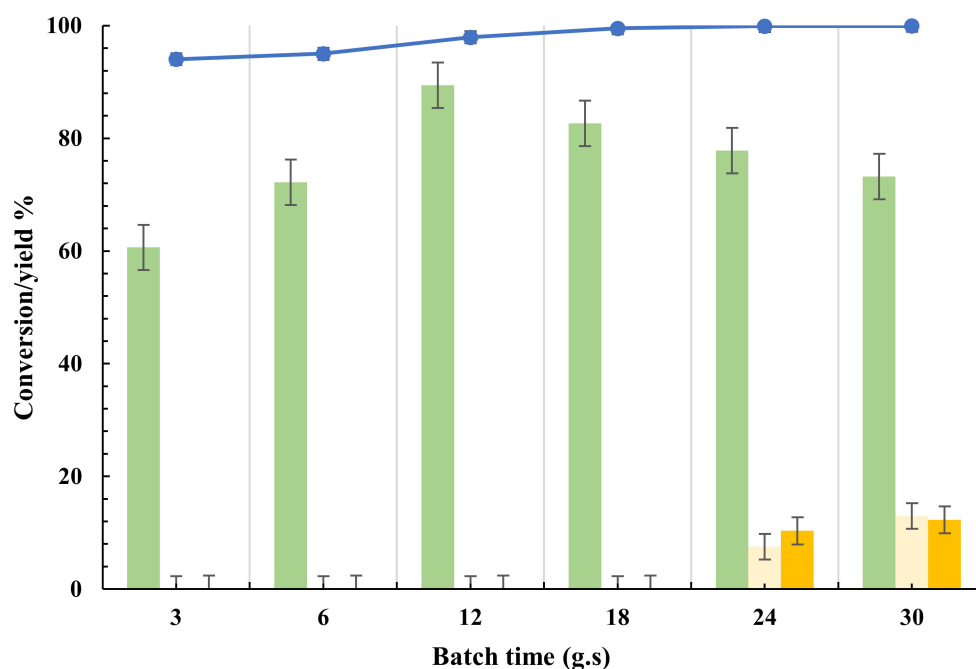


Figure 1. The effect of reaction batch time on product distribution via MW for fructose dehydration. Reaction conditions: MW via the standard power mode, 160 °C, 10 mg MIL-101(Cr)-SO₃H(3) ([H⁺] 0.009 mmol), 160 °C, 3 mL DMSO/acetone (70:30), catalyst/substrate = 0.3. (—) denotes fructose conversion %, (■) denotes 5-HMF yield %, (■) denotes FA yield %, and (■) denotes LA yield %. Error bars represent a 95% confidence interval.

The microwave effect is hypothesized to arise from selective heating of MW-absorbing molecules, i.e., the sulfonic acid group in the catalyst, DMSO, and fructose. As such, at the molecular scale, temperature inhomogeneities could develop depending on the effectiveness of MW energy absorption and heat dissipation. Nevertheless, only a bulk medium temperature could be measured, and it can be reasonably assumed that no local excessive temperatures developed that would lead to significant humin formation and a decreasing furfural yield. The development of a model capable of simultaneously tracking the evolution of 5-HMF and other substances involved in the dehydration reaction during the reaction time will provide further insight into the MW effect. Accordingly, multiresponse modeling for the dehydration reaction was conducted.

2.2. Multiresponse Kinetic Modeling and Reaction Conditions Optimization

Selectivity towards 5-HMF in fructose dehydration was investigated over a wide range of operating conditions. More particularly, a series of representative experiments were performed to elucidate the impact of the heat supply method, i.e., conventional or microwave heating, on fructose dehydration kinetics. In addition to the experimentation, a kinetic modeling approach was also followed to probe the reaction rate enhancement. Such a model may provide an explanation for variations in the maximum 5-HMF yield at different reaction temperatures at specific times. Figure 2 shows a parity diagram of the three responses of all 63 data points of fructose dehydration carried out under CH and MW conditions and reveals that the kinetic model is able to satisfactorily reproduce the experimental trends of each component (fructose, 5-HMF, LA, and FA) within the investigated range of operating conditions.

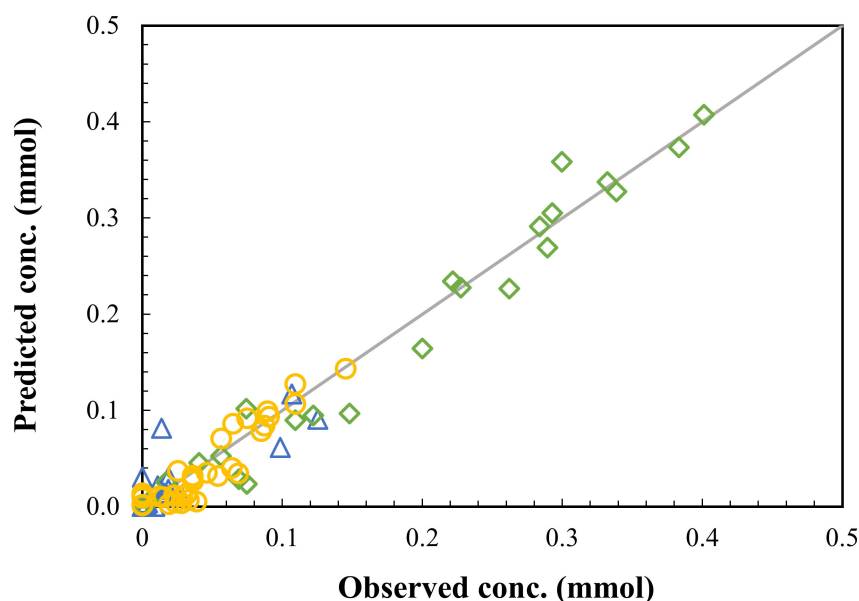
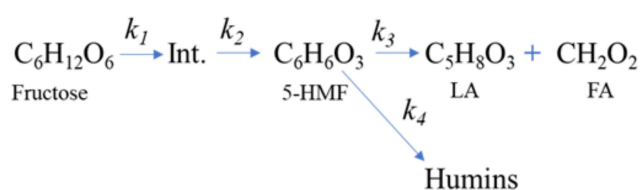


Figure 2. Parity diagram for all experimental and simulated points of fructose dehydration carried out under CH and MW conditions. (Δ) stands for fructose conversion, (\circ) denotes LA + FA, and (\square) denotes 5-HMF.

2.2.1. Pre-Exponential Factors and Activation Energies under CH Conditions

In the proposed reaction network shown in Scheme 2, an intermediate was included in the reaction network based on the observed trends in the experimental data to account for the ‘delay’ in 5-HMF formation after fructose conversion. With respect to the source of humin formation, it is clear from the almost instantaneous occurrence of fructose transformation reactions (including its dehydration to 5-HMF) and the slower humin formation that the latter cannot be formed principally from fructose. Rather, side product formation seemed to occur mainly in line with further 5-HMF conversion. Therefore, in order to not overly complicate the reaction network, 5-HMF was the only origin considered for humin formation.



Scheme 2. Reaction pathways of fructose dehydration.

The estimated activation entropies ΔS_i and energies $E_{i,a}$ for each step are summarized in Table 6. The corresponding rate coefficients at the reference temperature of 150 °C were calculated using the estimated values of ΔS_i and $E_{i,a}$ via Equation (9) (see Table 7). Fructose dehydration to the (unspecified) intermediate has a high rate coefficient (k_1), making it the fastest step among the consecutive reactions in the scheme. The rate coefficient for the subsequent conversion of the intermediate to 5-HMF (k_2) is about half of that for fructose conversion into the intermediate (k_1). The apparent activation energy for the former ($E_{2,a} = 103$ kJ/mol) is higher than for the latter ($E_{a,1} = 88$ kJ/mol), which implies that further intermediate conversion into 5-HMF more significantly depends on temperature. The higher (apparent) activation energy for the further conversion of the intermediate ($E_{2,a}$) may be attributed to the intermediate’s ring structure that prevents the preferred planar geometry around the $\text{C}=\text{O}^+$ group [116]. The intermediate’s structure is illustrated in Supplementary Materials S4, Scheme S1.

Table 6. Entropy change ΔS_i and apparent activation energy $E_{i,a}$, including 95% highest posterior density (HPD) intervals. obtained by Bayesian estimation against the CH dataset for fructose dehydration over MIL-101(Cr)-SO₃H(3).

Reaction Step	Entropy of Activation, ΔS_i [J/molK]	Activation Energy, $E_{i,a}$ [kJ/mol]
Fru \rightarrow Int.	-17.7 ± 1.4	88.0 ± 33.0
Int. \rightarrow 5-HMF	-25.8 ± 1.6	103.7 ± 43.0
5-HMF \rightarrow LA + FA	-63.2 ± 1.9	87.8 ± 45.0
5-HMF \rightarrow Humins	-38.2 ± 1.0	-
Microwave effect (ΔS_{MW} , ΔH_{MW})	16.8 ± 1.3	-87.5 ± 46.9

Table 7. Rate coefficients at 150 °C calculated using the values listed in Table 6 in Equations (1) and (9).

Reaction Step	Conventional Heating [mmol/min]	Microwave Conditions [mmol/min]
Fru \rightarrow Int.	$(1.0 \pm 0.002) \times 10^{-1}$	$(8.0 \pm 0.3) \times 10^{-1}$
Int. \rightarrow 5-HMF	$(4.6 \pm 0.3) \times 10^{-2}$	$(3.3 \pm 0.22) \times 10^{-1}$
5-HMF \rightarrow LA + FA	$(5.0 \pm 0.8) \times 10^{-3}$	$(3.3 \pm 7.4) \times 10^{-3}$
5-HMF \rightarrow Humins	$(9.0 \pm 0.3) \times 10^{-3}$	$(4.6 \pm 0.43) \times 10^{-2}$

Figure 3 shows the model simulations for CH at 140, 150, and 160 °C, as well as the experimentally obtained results at these temperatures. It can be observed that fructose dehydration to 5-HMF starts in the early minutes of heating. The maximum concentrations of the intermediate and 5-HMF are consecutively established, followed by degradation due to 5-HMF hydration to LA and FA and humin formation. Other side reactions may also occur with longer reaction times but are not considered specifically, i.e., their potential contribution is embedded in the considered humin formation [84,106,117]. At 140 °C and 150 °C (Figure 3a–f), 5-HMF yield reached its maximum values at 85 and 60 min, respectively. Overall, model simulations compared to experimental data for representative kinetic experiments of all experimental data indicate that the model describes experimental trends in CH reactors at various conditions (see Figure 3).

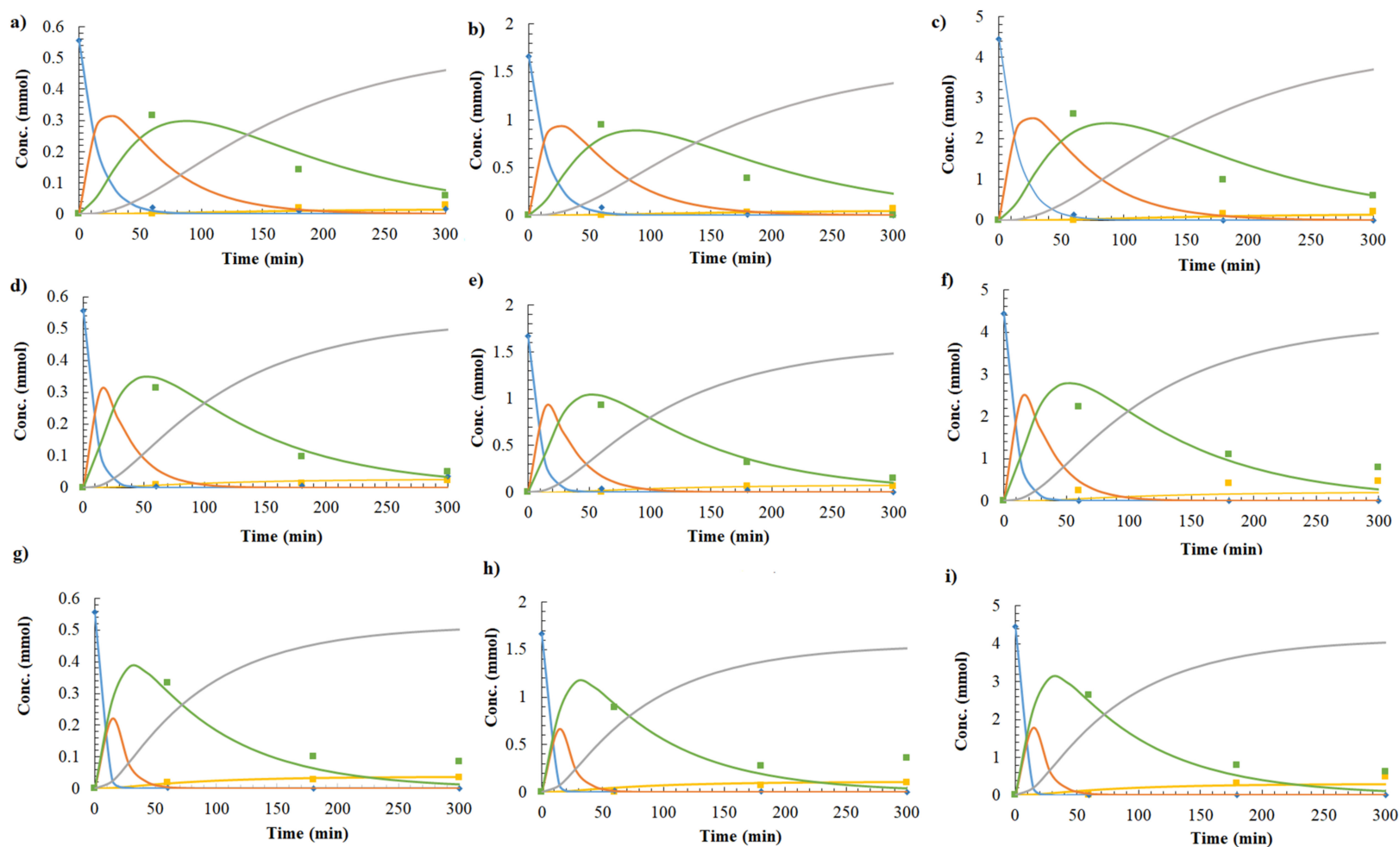


Figure 3. Kinetic model fit (lines) to the individually obtained experimental data. Typical time–concentration profile of the products of acid-catalyzed fructose dehydration at (a–c) 140 °C, (d–f) 150 °C, and (g–i) 160 °C for 100, 300, and 800 mg using CH heating with 3 mL solvent, 10 mg MIL-101(Cr)-SO₃H(3), and 100 mg fructose (0.56 mmol). Symbols denote experimental values: (■, —) fructose conversion, (○, —) intermediate formation, (■, —) 5-HMF production, (■, —) LA + FA production, (—) side product formation.

2.2.2. Quantification of the Microwave Irradiation Effect

It is essential to assess the origin of the reaction rate enhancements observed in the MW reactor. Thermal and non-thermal effects have been invoked in the literature for such an assessment [44,59,118]. The thermal effect of the MW is described to relate to dielectric heating that originates from polar molecules, e.g., the $-\text{SO}_3\text{H}$ of the catalyst and CH_2OH of fructose [119,120]. Those groups change their orientation at each alternation of the electric field, which creates friction and locally causes a different c.q. and higher temperature that results in an increased reaction rate. Secondary thermal phenomena such as conduction and convection inevitably occur, once again homogenizing temperature [119]. On the other hand, a specific MW effect, non-thermal in nature, is attributed to the rotational excitation of polar molecules and its impact on collision geometry and, hence, on the pre-exponential factor [62,63].

In the kinetic modeling, a homogeneous temperature distribution was considered, i.e., the implicit assumption that the dissipation of the absorbed MW energy via conduction and convection is fast compared to the reaction and eliminates any temperature difference. Additionally, the impact of MW irradiation on the Gibbs free energies of the transition states of the reaction steps was accounted for. Therefore, at MW conditions, two additional parameters occurred in the model, i.e., ΔH_{MW} and ΔS_{MW} (see Equation (1)).

$$k_n = \exp \frac{\Delta S_n + \Delta S_{\text{MW}}}{R} \times \exp \frac{-(E_{a,n} + \Delta H_{\text{MW}})}{R} \times \left(\frac{1}{T} - \frac{1}{T_{\text{avg}}} \right) \quad (1)$$

Of course, the impact of any potentially remaining residual local temperature difference is then embedded in this shift in Gibbs free energy as well. In summary, for parameter estimation for the MW series dataset, two parameters were added to each of the previously estimated values of ΔS_i and $E_{i,a}$ in the CH dataset, namely, ΔS_{MW} and ΔH_{MW} , respectively. Hence, the MW effect was calculated via a unique value applicable to the activation enthalpy and entropy for all considered reaction steps. For the sake of model simplicity, MW impact on all individual reaction steps was considered to be identical in the investigated temperature range compared to CH conditions. Accordingly, these parameters were used to quantify differences in thermochemical properties as they occurred under MW conditions for each rate coefficient (see Table 6).

The two additionally estimated ‘activation’ parameters for fructose conversion under MW conditions amounted to $16.8 \pm 1.3 \text{ J/mol/K}$ and $-87.5 \pm 46.9 \text{ kJ/mol}$ for ΔS_{MW} and ΔH_{MW} , respectively. Under MW, the apparent activation energy was significantly decreased. Furthermore, activation entropy became more positive. Hence, under MW conditions overall, the temperature dependence of the reaction rates is much less pronounced, which can be explained by considering that energy is brought into the reaction under a form other than heat. Yet, using a single Gibbs free energy adjustment for all considered reactions ensures that a limited temperature dependence of reaction rates remains.

It could be expected that the magnitude of the $-T\Delta S$ term would increase in an MW-induced reaction because of quick and random dipolar movement (dipolar polarization). Thus, microwave–molecules interactions increase the value of the second term in the Gibbs free energy equation. This hypothesis is evidenced by the change in ΔS_{MW} , which is attributed to the higher entropy generation in a microwave-assisted reaction and, hence, a higher pre-exponential factor due to a higher probability of collision. Moreover, the thermodynamic advantage provided by the MW is realized at lower temperatures where the free energy ($\Delta G = \Delta H - T\Delta S$) of the MW reaction becomes negative. The fact that the MW-driven reaction has a negative ΔG at lower temperatures than CH stems from its significantly lower value of ΔH . Therefore, at a lower temperature, a microwave-driven reaction will become more favorable than a CH reaction as $(-T\Delta S)_{\text{CH}} > (-T\Delta S)_{\text{MW}}$ (see Section 2.2.3).

These findings challenge the controversial MW non-thermal effect and the classical view of MW irradiation as only a heating method. Several demonstrative examples of quantifying the non-thermal effects were enumerated in support of this approach to justify

the reduction in activation energy under MW conditions [60,61,118,121]. Stiegman and coworkers investigated the dehydrogenation reaction of the steam–carbon process via MW and CH [118]. Their work indicated a significant MW-specific effect on the investigated reactions as the MW not only selectively heated the substrate, but also affected the primary thermokinetic steps of the reaction [118].

The rate coefficients under MW conditions at 150 °C are listed in Table 7. Comparatively, it is clear that the reaction is faster under MW irradiation than under CH in the investigated temperature range. Comparison of the rate coefficients shows a 7- to 10-fold enhancement in the reaction rate (e.g., k_1 and k_2), as shown in Table 7.

Performance profiles under MW conditions were simulated using the rate coefficients at 140, 150, and 160 °C, respectively (see Figures 4 and 5). As a result, it can be observed that the trends of 5-HMF, LA, and FA are qualitatively similar to those from the conversion of fructose under CH conditions, with the notable quantitative difference that the reaction occurred in a much shorter time under MW conditions, i.e., the rate of 5-HMF formation was faster under MW conditions. Nevertheless, many researchers still doubt whether reactions under MW conditions would occur according to the exact mechanisms that are exhibited under CH conditions [61,122].

Generally, at 140 °C, 150 °C, and 160 °C, MW conditions significantly promoted the consumption rate of fructose to form the intermediate, and higher 5-HMF yields were thus obtained within a shorter time. At 170 °C, more intermediate was formed, and less 5-HMF and other side products were detected (see Figure 6 for a better comparison). Consequently, the decrease in 5-HMF selectivity at 170 °C after 15 min can be attributed to 5-HMF hydration reactions that form LA and FA. This behavior can be explained by the interplay between the rate coefficients of consecutive reactions and the products' concentration. Since it functions as a "trigger" for enhancing one of the successive reactions from another, this in turn determines how the final concentrations of its components change as the reaction proceeds.

Figure 6a displays the formed intermediate's concentration at each temperature and how it is consumed in consecutive reactions, thus leading to 5-HMF formation, hydration, and self-oligomerization (Figure 6b–d, respectively). The interplay between the rate coefficients of the consecutive reactions and product concentrations functions as a "trigger" that enhances one of the consecutive reactions more than the other. In turn, this determines how the concentrations of its components change as the reaction proceeds. For example, under a given set of conditions (such as 160 °C), when the intermediate concentration is low, the reaction follows the direction that produces 5-HMF, leading to a relatively high 5-HMF yield and low side product yield.

To further evaluate the reliability of the developed kinetic model, a comparison of the estimated activation energies for main reactions between this study and previous studies using MIL-101(Cr) and other heterogeneous acid catalysts was conducted and is listed in Section S6 of the Supplementary Materials (see Table S2 in Section S6). Many prior studies have considered direct fructose conversion to 5-HMF without considering the intermediary step; thus, some parameters are expected to deviate from previously reported ones [84,123,124]. Still, models investigated previously include the same general reactions as the present work: fructose dehydration, 5-HMF hydration to levulinic acid and formic acid, and humin production from fructose and/or 5-HMF. Thus, some comparison is still possible. For example, Chen et al. [84] reported a kinetic study on fructose dehydration using MIL-101(Cr)-SO₃H in DMSO in the temperature range of 120–150 °C with a first-order approach (Table S2 Entry 4). The proposed reaction scheme only considered the rate of fructose conversion without other products, thus the intermediate and its concentration were not included in the model. As a result, the apparent activating energy amounted to $E = 55 \pm 5$ kJ/mol (Entry 4). To better compare our results to the prior work, a regression of the CH dataset was also performed without considering the intermediate in the reaction scheme (Table S2, Entry 3). In that case, the apparent activation energy for fructose dehydration was estimated at $E = 48 \pm 2$ kJ/mol (Table S2, Entry 3).

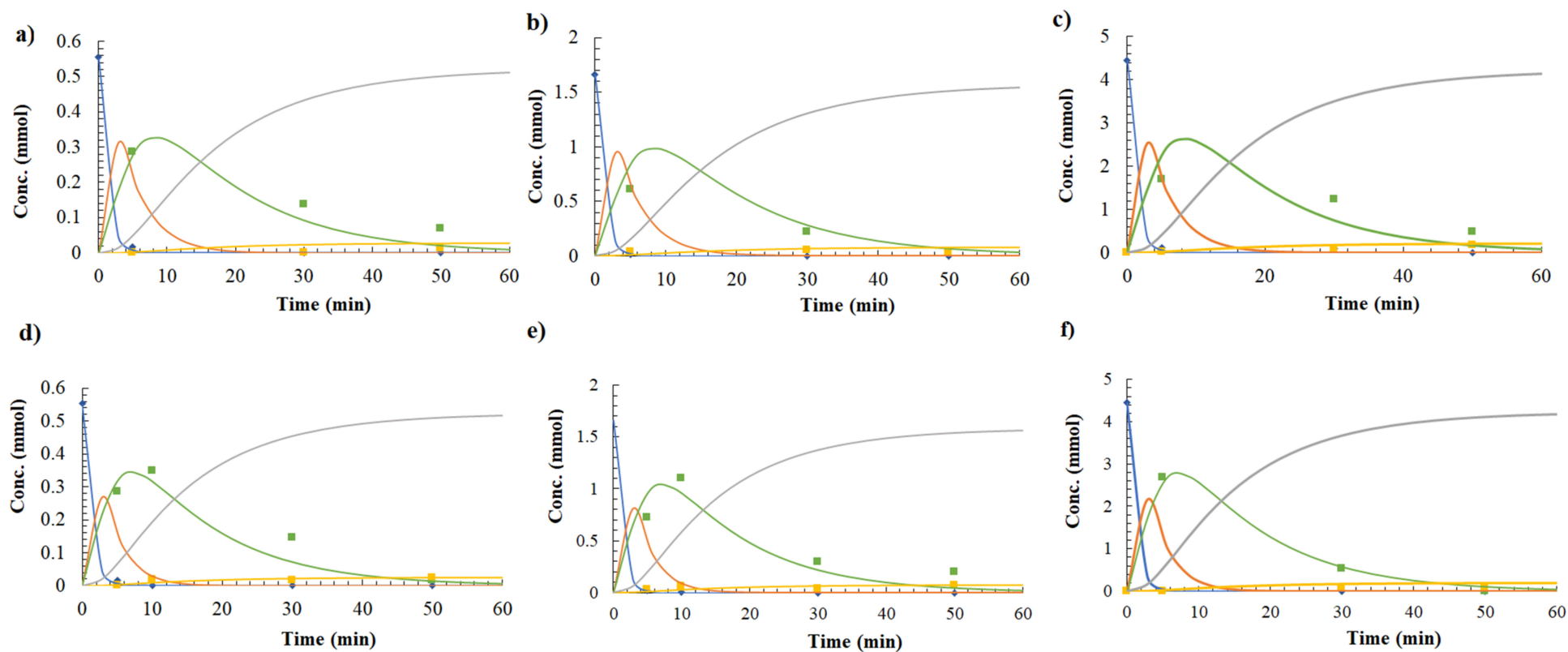


Figure 4. Performance profile of the products of acid-catalyzed fructose dehydration at (a–c) 140 °C and (d–f) 150 °C for 100, 300, and 800 mg under MW conditions with 3 mL solvent, 10 mg MIL-101(Cr)-SO₃H(3), and 100 mg fructose (0.56 mmol). Symbols denote experimental values: (■, —) fructose conversion, (—) intermediate formation, (■, —) 5-HMF production, (■, —) LA + FA production, (—) side product formation.

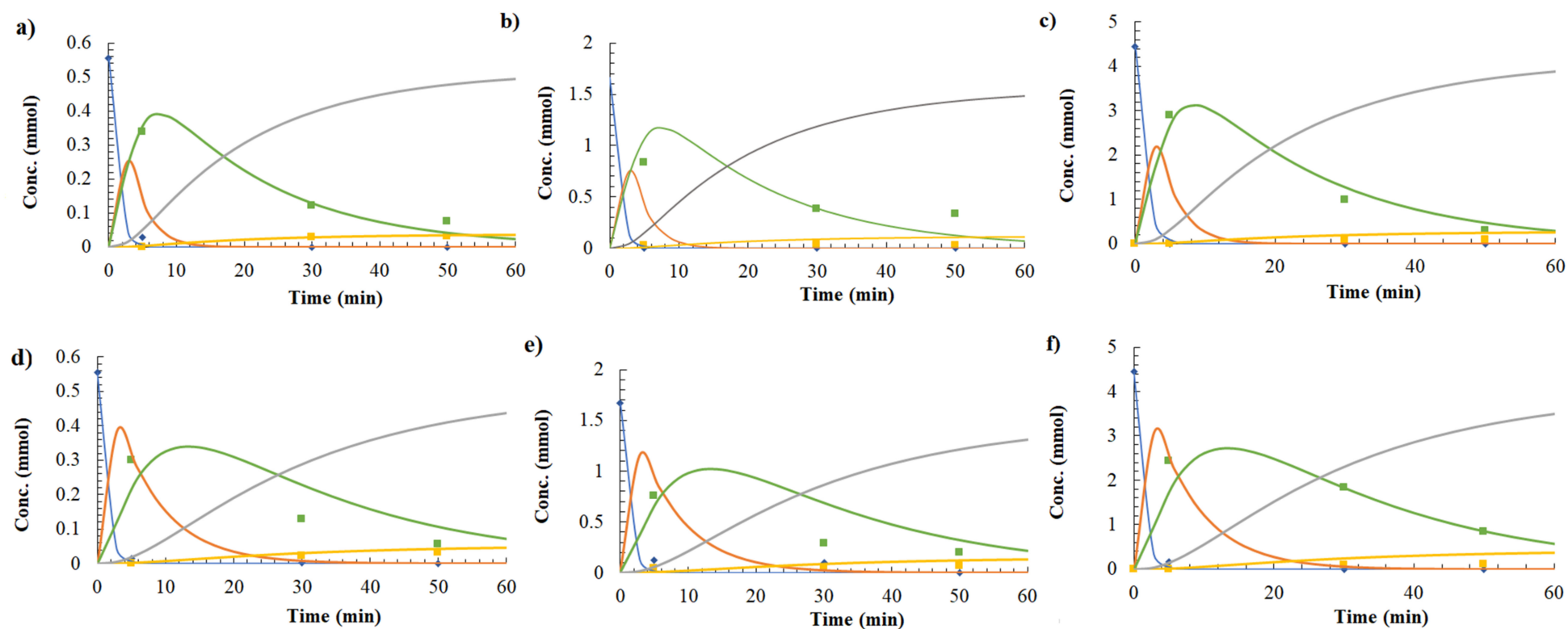


Figure 5. Performance profile of the products of acid-catalyzed fructose dehydration at (a–c) 160 °C and (d–f) 170 °C for 100, 300, and 800 mg using MW heating with 3 mL solvent, 10 mg MIL-101(Cr)-SO₃H(3), and 100 mg fructose (0.56 mmol). Symbols denote experimental values: (■, —) fructose conversion, (—) intermediate formation, (■, —) 5-HMF production, (■, —) LA + FA production, (—) side product formation.

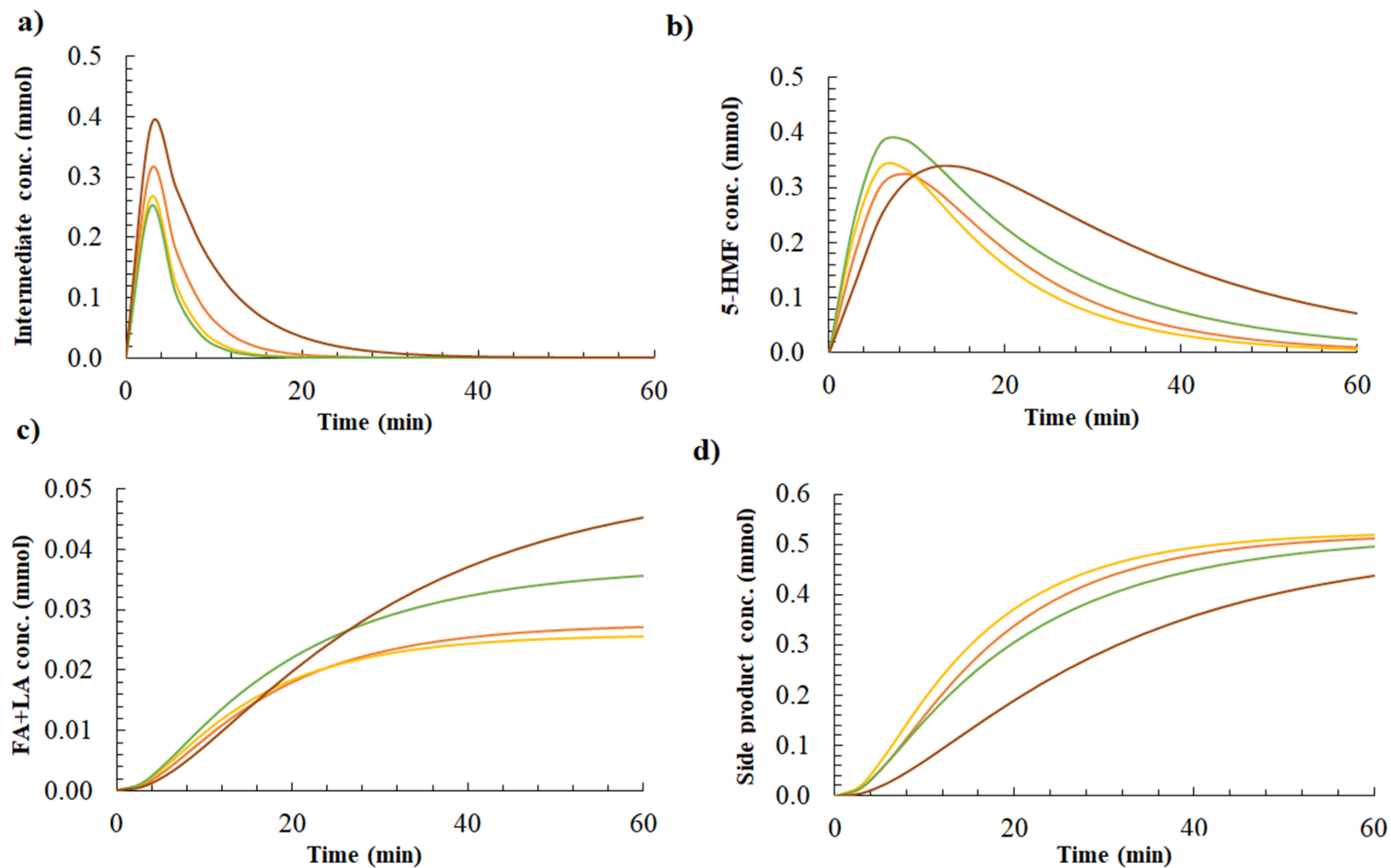


Figure 6. Predicted concentration profiles of acid-catalyzed fructose dehydration using MW heating: (a) intermediate formation, (b) 5-HMF production, (c) LA + FA production, (d) side product formation. Symbols denote simulated values at (—) 140 °C, (—) 150 °C, (—) 160 °C, and (—) 170 °C with 3 mL solvent, 10 mg MIL-101(Cr)-SO₃H(3), and 100 mg fructose (0.56 mmol).

Therefore, a model that does not account for the intermediate considered in our work would effectively lead to an (apparent) activation energy within this lower range of values. Hence, the observed deviations in reaction rates and activation energies between the results obtained from this work and those reported in the literature for the same catalyst are primarily ascribed to the different reaction networks proposed (Table S2, Entry 1–4).

Villanueva et al. investigated the kinetics of fructose conversion using ZrPO-700 as a catalyst at 125–145 °C (Table S2, Entry 5) [125]. The model was constructed using a similar reaction network to the one proposed in this work involving the conversion of fructose to a common intermediate, which was subsequently converted to 5-HMF before 5-HMF hydration to LA and FA. In parallel, fructose individually reacts to humins. The obtained activation energy for fructose conversion to this intermediate amounted to 186 kJ/mol (Entry 5), while the value obtained in this work was 88 kJ/mol (Table S2, Entry 1), indicating a significant dependence on the catalyst.

2.2.3. Maximum 5-HMF Yield as a Function of Temperature

The temperature dependence of the dehydration of fructose over MIL-101(Cr)-SO₃H was explored using the developed model. Generally, the production of 5-HMF requires elevated temperatures (>100 °C), which can be supplied by MW irradiation or CH. However, undesirable side reactions to humins are more favored at higher temperatures. Therefore, the dehydration of fructose to 5-HMF as a function of reaction time was simulated in a temperature range of 140 °C to 170 °C. The maximum simulated 5-HMF yields were plotted vs. reaction temperature for MW and CH conditions (see Figure 7).

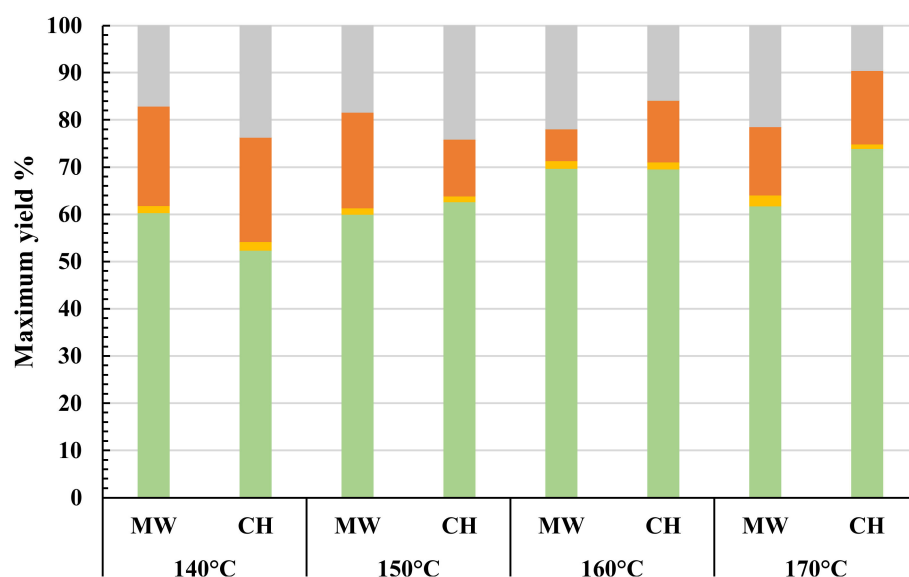


Figure 7. Temperature effect on the simulated maximum 5-HMF yield using MW heating for 10 min and CH for 90 min. The parameter estimates in the model correspond to the following conditions: 3 mL DMSO/acetone medium (70:30 *w/w*), 10 mg MIL-101(Cr)-SO₃H(3), and 100 mg fructose (0.56 mmol). (■) represents 5-HMF yield %, (■) represents FA + LA yield %, (■) represents intermediate yield %, and (■) represents side product yield %.

For CH, an increase in temperature leads to a rise in the maximum 5-HMF yield from fructose though this was obtained over a longer reaction time than under MW conditions (Figure 7), indicating the higher activation energy for fructose dehydration under CH conditions. For example, 5-HMF yield increased from 54.3 to 70.1% under CH conditions by increasing the reaction temperature from 140 °C to 160 °C. The results showed that, at 170 °C, the highest yield of 5-HMF was achieved using CH (74.2%).

At 140 °C, more 5-HMF is generated under MW than under CH conditions. Based on the results, it is clear that the MW enhances selective conversion into 5-HMF at a

significantly lower temperature, making it more energy efficient. It was hinted before (Section 2.2.2) that as the temperature decreases, MW conditions would become more favorable than CH as $-(T\Delta S)_{CH} > -(T\Delta S)_{MW}$. Moreover, under MW conditions, a more negative ΔG will already be obtained at lower temperatures compared to CH conditions. This arises from the significantly lower value of ΔH [60]. This conclusion supports the findings that at a higher temperature, such as 170 °C, the obtained 5-HMF yield by CH is higher than under MW conditions. Therefore, it can be concluded that under MW conditions, temperatures exceeding 160 °C may accelerate side reactions of 5-HMF, leading to species such as humins [115,126]. It can be concluded that milder reaction conditions associated with reduced reaction time are the key advantages brought about by the use of MW conditions for MW-susceptible reactions.

To evaluate the potential for industrial-scale applications, it is important to consider the amount of fructose that can be processed. Therefore, simulations were conducted for different substrate quantities ranging from 100 to 800 mg of fructose in a DMSO/acetone (70/30) solvent mixture, which corresponded to catalyst-to-substrate ratios of 0.1, 0.03, and 0.01. It was observed that fructose conversion occurred rapidly under microwave conditions regardless of the fructose-to-catalyst ratio, which is consistent with previous findings [48]. Figure 8 illustrates the highest achievable dehydration yield under MW and CH conditions. As hinted before, a similar maximum 5-HMF yield in both reactors was obtained at different reaction times.

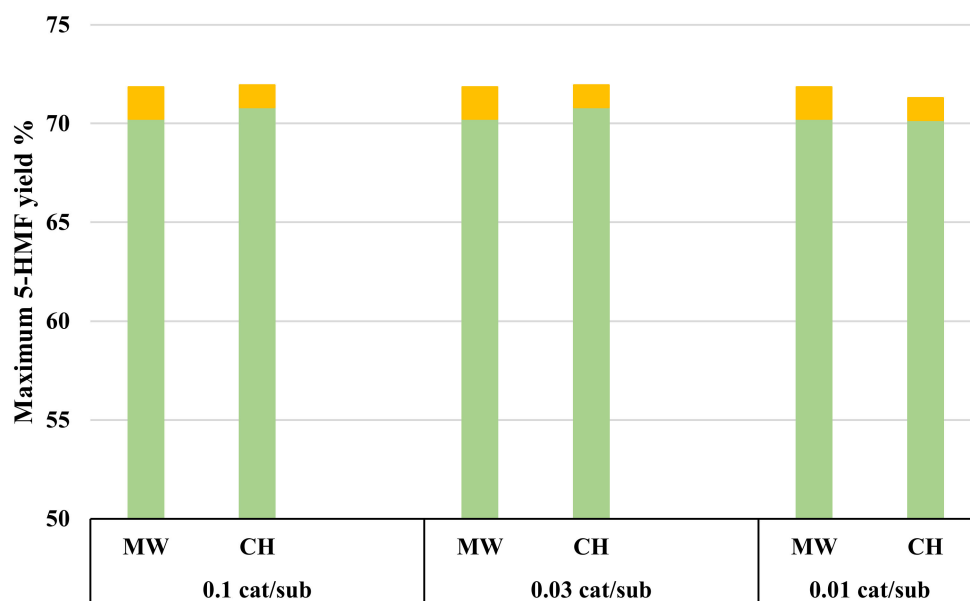


Figure 8. The effect of catalyst-to-substrate ratio on simulated maximum yields using MW heating for 10 min and CH for 90 min. The parameter estimates in the model correspond to the following conditions: 3 mL DMSO/acetone medium (70:30 *w/w*) and 10 mg MIL-101(Cr)-SO₃H(3) at 160 °C. (■) 5-HMF (mmol), (■) FA + LA (mmol).

Additionally, the results of experiments included in the Supplementary data (Section S7) indicate that selectivity towards 5-HMF remained stable as fructose concentration increased from 100 mg to 800 mg. This finding is consistent with the existing literature [127,128]. It is important to note that the impact of fructose concentration on 5-HMF selectivity can vary depending on the specific reaction conditions, including the catalyst type, reaction temperature, and reaction time.

3. Materials and Methods

3.1. Chemicals and Catalysts

Dimethyl sulfoxide (DMSO) ($C_2H_6OS \geq 99.9\%$, Sigma Aldrich, Saint Louis, MO, USA), acetone ($C_3H_6O \geq 99.5\%$, Acros Organics, Madrid, Spain), 5-hydroxymethylfurfural (5-HMF) ($C_6H_8O_3 \geq 99.5\%$, Sigma Aldrich, Saint Louis, MO, USA), D-fructose ($C_6H_{12}O_6 \geq 99\%$, Sigma Aldrich, Saint Louis, MO, USA), levulinic acid ($C_5H_8O_3 \geq 99.5\%$, Sigma Aldrich, Saint Louis, MO, USA), formic acid ($CH_2O_2 \geq 99.5\%$, Sigma Aldrich, Saint Louis, MO, USA), sulfuric acid ($H_2SO_4 \geq 98\%$, Sigma Aldrich, Saint Louis, MO, USA), hydrochloric acid ($HCl \geq 98\%$, Sigma Aldrich, Saint Louis, MO, USA), and HPLC water. Chemicals were used without further purification. Catalyst preparation has been described elsewhere [68].

3.2. Catalyst Testing

Two different heating methods, i.e., conventional heating (CH) and microwave (MW) heating, were used to produce 5-HMF from D-fructose. Both methods were performed and compared under similar conditions. Note that this comparison includes the difference in time required to reach the desired reaction temperature, which is much shorter when using MW heating. 5-HMF yield and selectivity were investigated in a fructose concentration and reaction temperature range of 0.1–0.8 g within 3 mL of solvent and from 140 to 170 °C, respectively. The reaction time for CH varied between 60 and 300 min, while the examined time range for MW heating was from 5 to 50 min. Before the reaction, the catalyst was pre-treated at 180 °C under vacuum for 4 h. This thermal activation under vacuum was employed to release solvent molecules, specifically water, and was coordinated to the chromium centers in MIL-101(Cr)-SO₃H. This process facilitated the liberation of the metal node and the creation of open chromium sites, which can be more readily accessed by potential reactants [129]. The absence of mass and heat transfer limitations for dehydration reaction over MIL-101(Cr)-SO₃H was confirmed by verifying the necessary criteria [82].

3.2.1. General Procedure for the Reaction of Fructose Using Microwave Irradiation

The catalytic tests involving microwave heating were performed with a Discover microwave reactor (CEM Corporation, Charlotte, NC, USA). The CEM Focused Microwave™ Synthesis System Discover® SP is designed to enhance the ability to perform chemical reactions under controlled conditions on the laboratory scale [130]. In a typical experiment for the transformation of fructose, a 10 mL reaction tube was charged with fructose, MIL-101(Cr)-SO₃H (10 mg), and solvent (3 mL); the reaction mixture was then heated to the desired temperature for the specified time. The 10 mL batch reaction vessel was placed in the center of the equipment for heating at 2450 MHz. In addition, a solenoid valve automatically released air jets over the surface of the flask to assist with temperature control. In all cases, the contents of reactors were magnetically stirred.

The standard power mode was examined as suggested by the manufacturer for the control of routine organic syntheses [130]. The reactor employs a feedback loop that automatically varies MW power to establish and maintain the desired temperature. In this mode, temperature and reaction time can be controlled; the temperature gradually increases to reach the set value (see Figure 9). Moreover, a short pre-heating or ramp time over the first 0–1 s was selected for all runs. The cooling option consists of the necessary valves and ports to direct a cooling gas (air) onto the vessel in the system cavity. Cooling will decrease the temperature of a 3 mL solution in a 10 mL reaction vessel from ~150 °C to ~50 °C in less than 120 s. Standard power mode pressure and power profiles are displayed in Supplementary Materials S1.

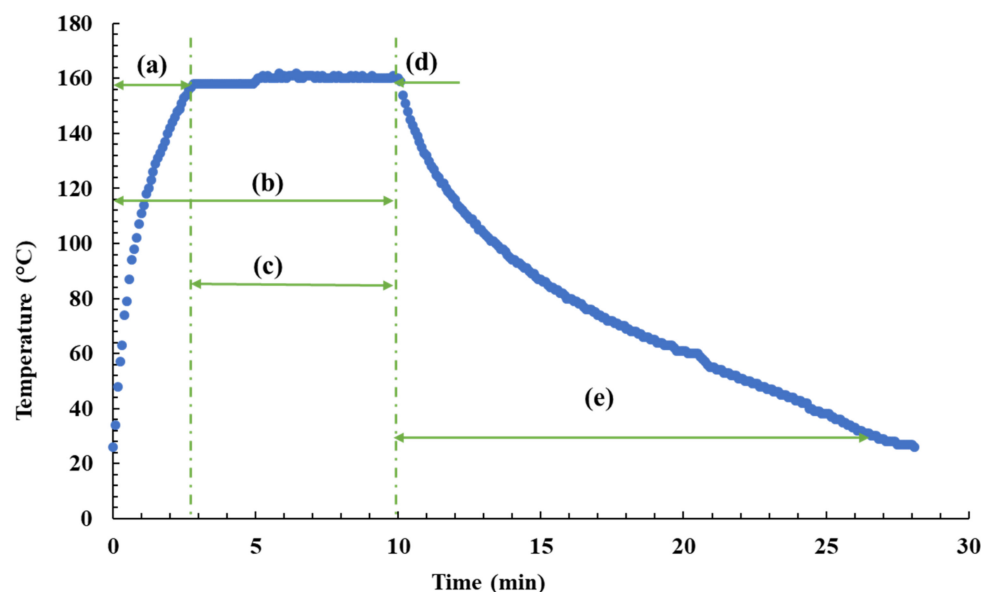


Figure 9. Temperature profile of a microwave irradiation experiment using the standard power mode: (a) ramp time or heating time (heating from an ambient temperature to the final reaction temperature over the first 0–1 min), (b) total time, (c) reaction time, (d) end of hold reaction time at the desired reaction temperature, and (e) heat dissipation time without power supply.

3.2.2. General Procedure for the Dehydration Reaction of Fructose Using Conventional Heating

A round-bottom glass flask equipped with a magnetic bar was charged with fructose, catalyst, and solvent and was then placed in a pre-heated oil bath at the desired temperature. The temperature was kept at the desired value, which ranged from 140 to 170 °C. A time of 10 to 12 min was needed for the oil bath to reach the set temperature.

3.3. Analysis

The reaction mixture was analyzed using a Shimadzu high-performance liquid chromatography (HPLC) (Shimadzu LC-20AB, Kyoto, Japan). The instrument used for HPLC was equipped with a refractive index (RID) detector (in the range of 1.00–1.75), a photodiode array detector, and a Biorad Aminex HPX-87H column (Bio-Rad Laboratories N.V., Hercules, CA, USA). The RID detector was used to detect fructose, while 5-HMF, FA, and LA were individually detected on the UV detector at wavelengths of 355 nm, 211 nm, and 254 nm, respectively. A 0.005 M H₂SO₄ solution was used as the mobile phase at a flow rate of 0.6 mL/min, and the column temperature was maintained at 65 °C. The content of fructose, 5-HMF, levulinic acid (LA), and formic acid (FA) in samples was quantified from calibration curves established from the standard compounds. Fructose, FA, LA, and 5-HMF were eluted at 10, 13.1, 14.7, and 37.1 min, respectively. The typical relative standard error was 1% for multiple injections from the same sample and 5–8% for replicate samples during HPLC analysis. Reactant conversion, product yield, and selectivity were obtained by Equations (2)–(4):

$$\text{5-HMF yield [\%]} = \left(\frac{\text{moles of 5-HMF produced}}{\text{initial moles of fructose}} \right) \times 100 \quad (2)$$

$$\text{5-HMF selectivity [\%]} = \left(\frac{\text{moles of 5-HMF produced}}{\text{converted moles of fructose}} \right) \times 100 \quad (3)$$

$$\text{Fructose conversion [\%]} = \left(\frac{\text{converted moles of fructose}}{\text{Initial moles of fructose}} \right) \times 100 \quad (4)$$

The yields of FA and LA are calculated in an analogous manner to 5-HMF. For detailed information regarding the quantification of the reaction products, see Supplementary Materials S2. Due to HPLC lacking the ability to detect humins, their quantification was performed by employing the carbon mass balance method, which accounts for the total quantities of 5-HMF, LA, and FA.

3.4. Procedure for Multiresponse Kinetic Modeling

Apart from the experimental assessment, the effect of microwaves in fructose transformation into 5-HMF was also quantified by multiresponse kinetic modeling. The kinetic parameters, including those employed to capture the 'microwave effect', were determined by regression against a total of 63 experimental data points, i.e., 27 using CH and 36 using MW irradiation. Simultaneous regressions were run for CH and MW heating.

The kinetics of the reaction presented in Scheme 1 has been assessed by making use of the reaction network in Scheme 2. One of its key features is that fructose conversion occurs via an intermediate (Int.) (see Section 2.2), which subsequently gets converted into 5-HMF. Upon further transformation, the latter can decompose into FA and LA and can lead to the possible formation of side products such as humins. The following simplifying assumptions were made when developing the kinetic model: (i) all reactions are irreversible and first-order and (ii) humins are predominantly formed from 5-HMF. The latter assumption was made as distinguishing the source of humin formation was impossible and to avoid over-parameterization of the model.

Each reaction step was assigned a rate coefficient (k). Finally, the reaction network was translated into a mathematical model by setting up differential equations for each reaction step as they occurred within the batch reactor. As presented in Scheme 2, this reaction network yielded four ordinary differential equations and included multiple concentration responses (Equations (5)–(8)). This set of differential equations was simultaneously integrated over the experimental reaction time (time interval 'c' in Figure 9) using the Athena Visual Studio engineering software.

$$\frac{dC_{\text{fru}}}{dt} = -k_1 C_{\text{fru}} \quad (5)$$

$$\frac{dC_{\text{Int.}}}{dt} = k_1 C_{\text{fru}} - k_2 C_{\text{Int.}} \quad (6)$$

$$\frac{dC_{\text{5-HMF}}}{dt} = k_2 C_{\text{Int.}} - k_3 C_{\text{5-HMF}} - k_4 C_{\text{5-HMF}} \quad (7)$$

$$\frac{dC_4}{dt} = k_3 C_{\text{5-HMF}} \quad (8)$$

In the expressions, the rate coefficients are calculated in a reparameterized manner (Equation (9)) [131]:

$$k_n = \exp \frac{\Delta S_n}{R} \times \exp \frac{-E}{R} \times \left(\frac{1}{T} - \frac{1}{T_{\text{avg}}} \right) \quad (9)$$

The model accounts for MW irradiation via a change in Gibbs free energy between the reactants and the activated complex, i.e., ΔG_{CH} and ΔG_{MW} ($\Delta G = \Delta H - T\Delta S$). Refer to Section 2.2.2 for the relevant assumptions. The Bayesian estimation method was used, which considers the error covariance matrix between responses and aligns the objective function accordingly [132]. The kinetic model was evaluated with the estimated parameters' highest posterior density (HPD) intervals.

4. Conclusions

In this work, a microwave-responsive catalyst was used in the assessment of fructose dehydration kinetics to 5-HMF over a MIL101(Cr)-SO₃H(3) catalyst comprising polar sulfonic acid groups in addition to the inherently available Cr⁺³ with coordinatively unsaturated sites. Due to intense rotations of the active site and the response of the polar

solvent in the microwave field, the reactivity is enhanced and the total reaction time is significantly reduced. For example, the 5-HMF yield obtained by the highly sulfonated-functionalized MIL-101(Cr) (MIL-101(Cr)-SO₃H(3)) is seven times higher than the parent MOF (MIL-101(Cr) in DMSO/acetone (70:30)).

The microwave effect was accounted for in the kinetic model (i) implicitly, through the rapid heating of the reaction mixture, as well as (ii) explicitly, through a difference in Gibbs free energy, thus accounting for the impact of the MW on activation entropy and enthalpy. MW conditions render activation entropy more positive by 16.7 J/mol, while only a marginal temperature dependence (activation energy) remained for the reaction steps. As a result, significant rate enhancements and shorter reaction times than CH were observed under MW conditions. Ultimately, the use of MW heating reduced the temperature required to drive the dehydration reactions into 5-HMF production and thus reduced side reactions that lower 5-HMF yield.

On a more generic level, by merging microwave-responsive catalysts such as MOFs with contemporary MW technology, a change in kinetic properties can be marked, leading to an enhancement in the selective substrate conversion rate. The low activation energy suggested that MW heating may be more promising than CH for biomass conversion, as demonstrated in this work for fructose dehydration. Taken together, the results suggest that a rational approach to the development of catalysts specifically for microwave-driven processes is advantageous to enhancing the utility of MW heating above current practices.

Supplementary Materials: The following supporting information can be downloaded at: <https://www.mdpi.com/article/10.3390/catal13030622/s1>, Figure S1: Typical microwave power (W) profile as a function of time (s); Figure S2: Typical microwave pressure (bar) profile as a function of time (s); Figure S3: HPLC chromatogram of fructose, FA, LA, and 5-HMF; Figure S4: HPLC calibration curve of fructose, FA, LA, and 5-HMF; Figure S5: Representation of DMSO molecule and thermal microwave effect where the induced microwave-irradiation; Figure S6: Post reaction mixture of fructose dehydration. Scheme S1: Proposed mechanism of glucose isomerization followed by fructose dehydration to 5-HMF over bifunctional MOF, MIL-101 SO₃H; Table S1: Heating profile data for fructose dehydration in MW reactor; Table S2: Overview of the reported kinetic models on sugar dehydration over heterogeneous catalysts compared to this work; Table S3: The effect of the initial fructose concentration on 5-HMF selectivity. References [84,85,95,124,125,127] are cited in the Supplementary Materials.

Author Contributions: Conceptualization, N.A., J.L., P.M.H. and J.W.T.; methodology, N.A. and J.L., formal analysis, N.A., J.L., P.M.H. and J.W.T.; investigation, N.A., J.L., B.B., F.V., P.M.H. and J.W.T.; resources, P.M.H. and J.W.T.; data curation, N.A. and J.L.; writing—original draft preparation, N.A.; writing—review and editing, J.L., B.B., F.V., P.M.H. and J.W.T.; visualization, N.A., J.L. and J.W.T.; supervision, J.L., P.M.H. and J.W.T.; project administration, J.W.T.; funding acquisition, P.M.H. and J.W.T. All authors have read and agreed to the published version of the manuscript.

Funding: The authors gratefully acknowledge the financial support of the Flemish Government and Flanders Innovation & Entrepreneurship (VLAIO) through the Moonshot project NIBCON (HBC.2019.0117). B.B. thanks the Special Research Fund (BOF) of Ghent University (01D33318). J.L. acknowledges the Research Foundation—Flanders (FWO) for financial support through Grant Number 12Z2221N. P.M.H. would like to thank the Research and Development Program of Ghent University Global Campus (GUGC), Korea.

Data Availability Statement: Data is contained within the manuscript and Supplementary information.

Conflicts of Interest: The authors declare no conflict of interest.

Abbreviations and Acronyms

A	pre-exponential factor	min^{-1}
Ac	acetone	
avg	average	
b	bulk	
cat	catalyst	
CH	conventional heating	
DMSO	dimethyl sulfoxide	
$E_{i,a}$	activation energy	$\text{kJ}\cdot\text{mol}^{-1}$
EL	ethyl levulinate	
EMF	5-ethoxymethylfurfural	
FA	formic acid	
FDCA	2,5-furandicarboxylic acid	
fru	fructose	
GVL	γ -valerolactone	
H	enthalpy	$\text{kJ}\cdot\text{mol}^{-1}$
HMF	hydroxymethylfurfural	
HPD	highest posterior density	
HPLC	high-performance liquid chromatography	
Int.	intermediate	
k	reaction rate constant for fructose dehydration	$\text{Mmol}\cdot\text{min}^{-1}$
LA	levulinic acid	
MIL	material of the Institute Lavoisier	
MW	microwave	
R	universal gas constant	$\text{J}\cdot\text{mol}^{-1}\text{K}^{-1}$
RID	refractive index detector	
SPCs	secondary building units	
S	entropy	$\text{J}\cdot\text{mol}^{-1}\text{K}^{-1}$
sub	substrate	
t	time	min
T	temperature	K
x	conversion	$\text{mol}\cdot\text{mol}^{-1}$
δ	tangent delta	
ϵ	dielectric constant	
ϵ''	dielectric loss	

References

- Aljammal, N.; Jabbour, C.; Thybaut, J.W.; Demeestere, K.; Verpoort, F.; Heynderickx, P.M. Metal-Organic Frameworks as Catalysts for Sugar Conversion into Platform Chemicals: State-of-the-Art and Prospects. *Coord. Chem. Rev.* **2019**, *401*, 213064. [[CrossRef](#)]
- Heidenreich, S.; Müller, M.; Foscolo, P.U. Biomass Pretreatment. In *Advanced Biomass Gasification; New Concepts for Efficiency Increase and Product Flexibility*; Elsevier: Amsterdam, The Netherlands, 2016; pp. 11–17, ISBN 9780128042960.
- Bozell, J.J.; Petersen, G.R. Technology Development for the Production of Biobased Products from Biorefinery Carbohydrates—The US Department of Energy’s “Top 10” Revisited. *Green Chem.* **2010**, *12*, 539–555. [[CrossRef](#)]
- Kuster, B.F.M. 5-Hydroxymethylfurfural (HMF). A Review Focussing on Its Manufacture. *Starch-Stärke* **1990**, *42*, 314–321. [[CrossRef](#)]
- Lewkowsky, J. Synthesis, Chemistry and Applications of 5-Hydroxymethyl-Furfural and Its Derivatives. *Arkivoc* **2001**, *2001*, 17–54. [[CrossRef](#)]
- Tahvildari, K.; Taghvaei, S.; Nozari, M. The Study of Hydroxymethylfurfural as a Basic Reagent for Liquid Alkanes Fuel Manufacture from Agricultural Wastes. *Int. J. Chem. Environ. Eng.* **2011**, *2*, 62–68.
- Fulignati, S.; Antonetti, C.; Tabanelli, T.; Cavani, F.; Raspolli Galletti, A.M. Integrated Cascade Process for the Catalytic Conversion of 5-Hydroxymethylfurfural to Furanic and TetrahydrofuranicDiethers as Potential Biofuels. *ChemSusChem* **2022**, *15*, e202200241. [[CrossRef](#)]
- Tong, X.; Ma, Y.; Li, Y. Biomass into Chemicals: Conversion of Sugars to Furan Derivatives by Catalytic Processes. *Appl. Catal. A Gen.* **2010**, *385*, 1–13. [[CrossRef](#)]
- Noppadon, S.; Allendorf, M.D.; George, A.; Jansen, R.; Leong, K.; Simmons, B.A.; Singh, S.; Travisano, P. Metal Organic Frameworks for the Conversion of Lignocellulosic Derivatives to Renewable Platform Chemicals 2019. US20190062293A1, 28 February 2019.

10. Nainamalai Devarajan and Palaniswamy Suresh MIL-101-SO₃H Metal-Organic Framework as a Brønsted Acid Catalyst in Hantzsch Reaction: An Efficient and Sustainable Methodology for One-Pot Synthesis of 1,4-Dihydropyridine. *New J. Chem.* **2019**, *43*, 6806–6814. [[CrossRef](#)]
11. Guan, W.; Zhang, Y.; Wei, Y.; Li, B.; Feng, Y.; Yan, C.; Huo, P.; Yan, Y. Pickering HIPEs Derived Hierarchical Porous Nitrogen-Doped Carbon Supported Bimetallic AuPd Catalyst for Base-Free Aerobic Oxidation of HMF to FDCA in Water. *Fuel* **2020**, *278*, 118362. [[CrossRef](#)]
12. Martínez-Vargas, D.X.; Rivera De La Rosa, J.; Sandoval-Rangel, L.; Guzmán-Mar, J.L.; Garza-Navarro, M.A.; Lucio-Ortiz, C.J.; De Haro-Del Río, D.A. 5-Hydroxymethylfurfural Catalytic Oxidation under Mild Conditions by Co (II), Fe (III) and Cu (II) Salen Complexes Supported on SBA-15: Synthesis, Characterization and Activity. *Appl. Catal. A Gen.* **2017**, *547*, 132–145. [[CrossRef](#)]
13. Luo, W.; Sankar, M.; Beale, A.M.; He, Q.; Kiely, C.J.; Bruijninx, P.C.A.; Weckhuysen, B.M. High Performing and Stable Supported Nano-Alloys for the Catalytic Hydrogenation of Levulinic Acid to γ -Valerolactone. *Nat. Commun.* **2015**, *6*, 6540. [[CrossRef](#)]
14. Chen, J.; Zhao, G.; Chen, L. Efficient Production of 5-Hydroxymethylfurfural and Alkyl Levulinate from Biomass Carbohydrate Using Ionic Liquid-Based Polyoxometalate Salts. *RSC Adv.* **2014**, *4*, 4194–4202. [[CrossRef](#)]
15. Liu, A.; Zhang, Z.; Fang, Z.; Liu, B.; Huang, K. Synthesis of 5-Ethoxymethylfurfural from 5-Hydroxymethylfurfural and Fructose in Ethanol Catalyzed by MCM-41 Supported Phosphotungstic Acid. *J. Ind. Eng. Chem.* **2014**, *20*, 1977–1984. [[CrossRef](#)]
16. Ouyang, W.; Zhao, D.; Wang, Y.; Balu, A.M.; Len, C.; Luque, R. Continuous Flow Conversion of Biomass-Derived Methyl Levulinate into γ -Valerolactone Using Functional Metal Organic Frameworks. *ACS Sustain. Chem. Eng.* **2018**, *6*, 6746–6752. [[CrossRef](#)]
17. Horváth, I.T.; Mehdi, H.; Fábos, V.; Boda, L.; Mika, L.T. γ -Valerolactone—A Sustainable Liquid for Energy and Carbon-Based Chemicals. *Green Chem.* **2008**, *10*, 238–242. [[CrossRef](#)]
18. Huber, G.W.; Corma, A. Synergies between Bio- and Oil Refineries for the Production of Fuels from Biomass. *Angew. Chem. Int. Ed.* **2007**, *46*, 7184–7201. [[CrossRef](#)] [[PubMed](#)]
19. Insyani, R.; Verma, D.; Kim, S.M.; Kim, J. Direct One-Pot Conversion of Monosaccharides into High-Yield 2,5-Dimethylfuran over a Multifunctional Pd/Zr-Based Metal-Organic Framework@Sulfonated Graphene Oxide Catalyst. *Green Chem.* **2017**, *19*, 2482–2490. [[CrossRef](#)]
20. Fang, R.; Luque, R.; Li, Y. Efficient One-Pot Fructose to DFF Conversion Using Sulfonated Magnetically Separable MOF-Derived Fe₃O₄(111) Catalysts. *Green Chem.* **2017**, *19*, 647–655. [[CrossRef](#)]
21. Fang, R.; Luque, R.; Li, Y. Selective Aerobic Oxidation of Biomass-Derived HMF to 2,5-Diformylfuran Using a MOF-Derived Magnetic Hollow Fe-Co Nanocatalyst. *Green Chem.* **2016**, *18*, 3152–3157. [[CrossRef](#)]
22. Liu, R.; Chen, J.; Chen, L.; Guo, Y.; Zhong, J. One-Step Approach to 2,5-Diformylfuran from Fructose by Using a Bifunctional and Recyclable Acidic Polyoxometalate Catalyst. *Chempluschem* **2014**, *79*, 1448–1454. [[CrossRef](#)]
23. Tao, F.; Cui, Y.; Yang, P.; Gong, Y. One-Pot, One-Step, Catalytic Synthesis of 2,5-Diformylfuran from Fructose. *Russ. J. Phys. Chem. A* **2014**, *88*, 1091–1096. [[CrossRef](#)]
24. Zhang, F.; Liu, Y.; Yuan, F.; Niu, X.; Zhu, Y. Efficient Production of the Liquid Fuel 2,5-Dimethylfuran from 5-Hydroxymethylfurfural in the Absence of Acid Additive over Bimetallic PdAu Supported on Graphitized Carbon. *Energy Fuels* **2017**, *31*, 6364–6373. [[CrossRef](#)]
25. Choudhary, V.; Mushrif, S.H.; Ho, C.; Anderko, A.; Nikolakis, V.; Marinkovic, N.S.; Frenkel, A.I.; Sandler, S.I.; Vlachos, D.G. Insights into the Interplay of Lewis and Brønsted Acid Catalysts in Glucose and Fructose Conversion to 5-(Hydroxymethyl)Furfural and Levulinic Acid in Aqueous Media. *J. Am. Chem. Soc.* **2013**, *135*, 3997–4006. [[CrossRef](#)]
26. Yang, F.; Liu, Q.; Bai, X.; Du, Y. Conversion of Biomass into 5-Hydroxymethylfurfural Using Solid Acid Catalyst. *Bioresour. Technol.* **2011**, *102*, 3424–3429. [[CrossRef](#)]
27. Tao, F.; Song, H.; Chou, L. Dehydration of Fructose into 5-Hydroxymethylfurfural in Acidic Ionic Liquids. *RSC Adv.* **2011**, *1*, 672–676. [[CrossRef](#)]
28. Steinbach, D.; Kruse, A.; Sauer, J.; Vetter, P. Sucrose Is a Promising Feedstock for the Synthesis of the Platform Chemical Hydroxymethylfurfural. *Energies* **2018**, *11*, 645. [[CrossRef](#)]
29. Zhou, C.; Zhao, J.; Yagoub, A.E.G.A.; Ma, H.; Yu, X.; Hu, J.; Bao, X.; Liu, S. Conversion of Glucose into 5-Hydroxymethylfurfural in Different Solvents and Catalysts: Reaction Kinetics and Mechanism. *Egypt. J. Pet.* **2017**, *26*, 477–487. [[CrossRef](#)]
30. Li, Q.; Zhuo, Y.; Shanks, K.; Taylor, R.A.; Conneely, B.; Tan, A.; Shen, Y.; Scott, J. A Winged Solar Biomass Reactor for Producing 5-Hydroxymethylfurfural (5-HMF). *Sol. Energy* **2021**, *218*, 455–468. [[CrossRef](#)]
31. Jia, S.; He, X.; Xu, Z. Valorization of an Underused Sugar Derived from Hemicellulose: Efficient Synthesis of 5-Hydroxymethylfurfural from Mannose with Aluminum Salt Catalyst in Dimethyl Sulfoxide/Water Mixed Solvent. *RSC Adv.* **2017**, *7*, 39221–39227. [[CrossRef](#)]
32. Menegazzo, F.; Ghedini, E.; Signoretto, M. 5-Hydroxymethylfurfural (HMF) Production from Real Biomasses. *Molecules* **2018**, *23*, 2201. [[CrossRef](#)]
33. Sansuk, S.; Subsadsana, M. Synthesis of 5-Hydroxymethylfurfural from Glucose Using H-Beta Catalyst Treated with Phosphoric Acid in One-Pot Biphasic Solvent System. *Energy Sources Part A Recover. Util. Environ. Eff.* **2019**, *41*, 2769–2777. [[CrossRef](#)]
34. Zhang, Y.; Pidko, E.A.; Hensen, E.J.M. Molecular Aspects of Glucose Dehydration by Chromium Chlorides in Ionic Liquids. *Chem. A Eur. J.* **2011**, *17*, 5281–5288. [[CrossRef](#)]
35. Sheldon, R.A. Green Solvents for Sustainable Organic Synthesis: State of the Art. *Green Chem.* **2005**, *7*, 267–278. [[CrossRef](#)]

36. Richel, A.; Paquot, M. Conversion of Carbohydrates under Microwave Heating. In *Carbohydrates-Comprehensive Studies on Glycobiology and Glycotechnology*; IntechOpen: London, UK, 2012.
37. Hu, D.; Zhang, M.; Xu, H.; Wang, Y.; Yan, K. Recent Advance on the Catalytic System for Efficient Production of Biomass-Derived 5-Hydroxymethylfurfural. *Renew. Sustain. Energy Rev.* **2021**, *147*, 111253. [[CrossRef](#)]
38. Flores, E.M.M.; Cravotto, G.; Bizzi, C.A.; Santos, D.; Iop, G.D. Ultrasound-Assisted Biomass Valorization to Industrial Interesting Products: State-of-the-Art, Perspectives and Challenges. *Ultrason. Sonochem.* **2021**, *72*, 105455. [[CrossRef](#)] [[PubMed](#)]
39. Fang, Z.; Smith, R.L.; Qi, X. *Production of Biofuels and Chemicals with Microwave*; Springer: Berlin/Heidelberg, Germany, 2015; Volume 3, ISBN 978-981-10-5136-4.
40. Siddique, I.J.; Salema, A.A.; Antunes, E.; Vinu, R. Recent Advance on the Catalytic System for Efficient Production of Biomass-Derived 5-Hydroxymethylfurfural. *Renew. Sustain. Energy Rev.* **2022**, *153*, 111767. [[CrossRef](#)]
41. Gude, V.G.; Patil, P.; Deng, S. Recent Advance on the Catalytic System for Efficient Production of Biomass-Derived 5-Hydroxymethylfurfural. In Proceedings of the World Renewable Energy Forum, WREF 2012, Including World Renewable Energy Congress XII and Colorado Renewable Energy Society (CRES) Annual Conference, Denver, CO, USA, 13–17 May 2012; Volume 1, pp. 751–759.
42. Leadbeater, N.E. *Microwave Heating as a Tool for Sustainable Chemistry*; CRC Press: Boca Raton, FL, USA, 2010; ISBN 9781439812709.
43. Gillespie, P.M. Microwave Chemistry—An Approach to the Assessment of Chemical Reaction Hazards. *ICHEME Symp. Ser. No* **2004**, *10*, 23–25.
44. Rosana, M.R.; Hunt, J.; Ferrari, A.; Southworth, T.A.; Tao, Y.; Stiegman, A.E.; Dudley, G.B. Microwave-Specific Acceleration of a Friedel-Crafts Reaction: Evidence for Selective Heating in Homogeneous Solution. *J. Org. Chem.* **2014**, *79*, 7437–7450. [[CrossRef](#)]
45. Guzik, P.; Kulawik, P.; Zając, M.; Migdał, W. Microwave Applications in the Food Industry: An Overview of Recent Developments. *Crit. Rev. Food Sci. Nutr.* **2021**, *62*, 7989–8008. [[CrossRef](#)]
46. Tabasso, S. Microwave-Assisted Biomass Conversion. In *Microwave Chemistry*; De Gruyter: Berlin, Germany, 2017; pp. 370–382, ISBN 9783110479935.
47. Kim, E.S.; Liu, S.; Abu-Omar, M.M.; Mosier, N.S. Selective Conversion of Biomass Hemicellulose to Furfural Using Maleic Acid with Microwave Heating. *Energy Fuels* **2012**, *26*, 1298–1304. [[CrossRef](#)]
48. Sweeygers, N. *The Microwave-Assisted Production of 5-Hydroxymethylfurfural and Furfural from Renewable Resources*; KU Leuven: Leuven, Belgium, 2019.
49. Hansen, T.S.; Woodley, J.M.; Riisager, A. Efficient Microwave-Assisted Synthesis of 5-Hydroxymethylfurfural from Concentrated Aqueous Fructose. *Carbohydr. Res.* **2009**, *344*, 2568–2572. [[CrossRef](#)] [[PubMed](#)]
50. Wei, R.; Wang, P.; Zhang, G.; Wang, N.; Zheng, T. Microwave-Responsive Catalysts for Wastewater Treatment: A Review. *Chem. Eng. J.* **2020**, *382*, 122781. [[CrossRef](#)]
51. Qin, M.; Zhang, L.; Wu, H. Dielectric Loss Mechanism in Electromagnetic Wave Absorbing Materials. *Adv. Sci.* **2022**, *9*, 2105553. [[CrossRef](#)]
52. Martín, Á.; Navarrete, A. Microwave-Assisted Process Intensification Techniques. *Curr. Opin. Green Sustain. Chem.* **2018**, *11*, 70–75. [[CrossRef](#)]
53. Hayes, B.L. *Microwave Synthesis, Chemistry at the Speed of Light*; CEM Corp: Charlotte, NC, USA, 2002.
54. Polshettiwar, V.; Varma, R.S. Microwave-Assisted Organic Synthesis and Transformations Using Benign Reaction Media. *Acc. Chem. Res.* **2008**, *41*, 629–639. [[CrossRef](#)]
55. Herrero, M.A.; Kremsner, J.M.; Kappe, C.O.; Graz, K.V.; Graz, A. Nonthermal Microwave Effects Revisited: On the Importance of Internal Temperature Monitoring and Agitation in Microwave Chemistry. *J. Org. Chem.* **2008**, *73*, 36–47. [[CrossRef](#)]
56. Kappe, C.O.; Pieber, B.; Dallinger, D. Microwave Effects in Organic Synthesis: Myth or Reality? *Angew. Chem. Int. Ed.* **2013**, *52*, 1088–1094. [[CrossRef](#)]
57. Kappe, C.O. Reply to the Correspondence on Microwave Effects in Organic Synthesis. *Angew. Chem. Int. Ed.* **2013**, *52*, 2–7. [[CrossRef](#)]
58. Dudley, G.B.; Stiegman, A.E.; Rosana, M.R. Correspondence on Microwave Effects in Organic Synthesis. *Angew. Chem. Int. Ed.* **2013**, *52*, 2–8. [[CrossRef](#)] [[PubMed](#)]
59. Chen, P.; Rosana, M.R.; Dudley, G.B.; Stiegman, A.E. Parameters Affecting the Microwave-Specific Acceleration of a Chemical Reaction. *JOC* **2014**, *79*, 7425–7436. [[CrossRef](#)]
60. Hunt, J.T. *Microwave Enhanced Gasification of Carbon*; Florida State University: Tallahassee, FL, USA, 2014.
61. Fini, A.; Breccia, A. Chemistry by Microwaves. *Pure Appl. Chem.* **1999**, *71*, 573–579. [[CrossRef](#)]
62. Perreux, L.; Loupy, A.; Alain, P. Nonthermal Effects of Microwaves in Organic Synthesis. In *Microwaves in Organic Synthesis*; John Wiley & Sons: Hoboken, NJ, USA, 2013; pp. 127–207.
63. Miklavc, A. Strong Acceleration of Chemical Reactions Occurring through the Effects of Rotational Excitation on Collision Geometry. *ChemPhysChem* **2001**, *2*, 552–555. [[CrossRef](#)]
64. Hu, J.; Wildfire, C.; Stiegman, A.E.; Dagle, R.A.; Shekhawat, D.; Abdelsayed, V.; Bai, X.; Tian, H.; Bogle, M.B.; Hsu, C.; et al. Microwave-Driven Heterogeneous Catalysis for Activation of Dinitrogen to Ammonia under Atmospheric Pressure. *Chem. Eng. J.* **2020**, *397*, 125388. [[CrossRef](#)]
65. Horikoshi, S.; Minagawa, T.; Tsubaki, S.; Onda, A.; Serpone, N. Is Selective Heating of the Sulfonic Acid Catalyst AC-SO₃H by Microwave Radiation Crucial in the Acid Hydrolysis of Cellulose to Glucose in Aqueous Media? *Catalysts* **2017**, *7*, 231. [[CrossRef](#)]

66. Zhang, X.; Hayward, D.O.; Mingos, D.M.P. Apparent Equilibrium Shifts and Hot-Spot Formation for Catalytic Reactions Induced by Microwave Dielectric Heating. *Chem. Commun.* **1999**, *11*, 975–976. [CrossRef]
67. Kokel, A.; Schäfer, C.; Török, B. Application of Microwave-Assisted Heterogeneous Catalysis in Sustainable Synthesis Design. *Green Chem.* **2017**, *19*, 3729–3751. [CrossRef]
68. Herbst, A.; Janiak, C. Selective Glucose Conversion to 5-Hydroxymethylfurfural (5-HMF) Instead of Levulinic Acid with MIL-101Cr MOF-Derivatives. *New J. Chem.* **2016**, *40*, 7958–7967. [CrossRef]
69. Herbst, A.; Janiak, C. MOF Catalysts in Biomass Upgrading towards Value-Added Fine Chemicals. *CrystEngComm* **2017**, *19*, 4092–4117. [CrossRef]
70. Oozeerally, R.; Ramkhalawan, S.D.K.; Burnett, D.L.; Tempelman, C.H.L.; Degirmenci, V. ZIF-8 Metal Organic Framework for the Conversion of Glucose to Fructose and 5-Hydroxymethyl Furfural. *Catalysts* **2019**, *9*, 812. [CrossRef]
71. Oozeerally, R.; Burnett, D.L.; Chamberlain, T.W.; Walton, R.I.; Degirmenci, V. Exceptionally Efficient and Recyclable Heterogeneous Metal–Organic Framework Catalyst for Glucose Isomerization in Water. *ChemCatChem* **2018**, *10*, 706–709. [CrossRef]
72. Pertiwi, R.; Oozeerally, R.; Burnett, D.L.; Chamberlain, T.W.; Cherkasov, N.; Walker, M.; Kashtiban, R.J.; Krisnandi, Y.K.; Degirmenci, V.; Walton, R.I. Replacement of Chromium by Non-Toxic Metals in Lewis-Acid MOFs: Assessment of Stability as Glucose Conversion Catalysts. *Catalysts* **2019**, *9*, 437. [CrossRef]
73. Deng, H.; Grunder, S.; Cordova, K.E.; Valente, C.; Furukawa, H.; Hmadeh, M.; Gándara, F.; Whalley, A.C.; Liu, Z.; Asahina, S.; et al. Large-Pore Apertures in a Series of Metal–Organic Frameworks. *Science* **2012**, *336*, 1018–1023. [CrossRef] [PubMed]
74. Tranchemontagne, D.J.; Ni, Z.; O’Keeffe, M.; Yaghi, O.M. Reticular Chemistry of Metal–Organic Polyhedra. *Angew. Chem. Int. Ed.* **2008**, *47*, 5136–5147. [CrossRef]
75. Kalmutzki, M.J.; Diercks, C.S.; Yaghi, O.M. Metal–Organic Frameworks for Water Harvesting from Air. *Adv. Mater.* **2018**, *30*, e1704304. [CrossRef] [PubMed]
76. Britt, D.; Tranchemontagne, D.; Yaghi, O.M. Metal–Organic Frameworks with High Capacity and Selectivity for Harmful Gases. *Proc. Natl. Acad. Sci. USA* **2008**, *105*, 11623–11627. [CrossRef] [PubMed]
77. Eddaoudi, M.; Kim, J.; Rosi, N.; Vodak, D.; Wachter, J.; O’Keeffe, M.; Yaghi, O.M. Systematic Design of Pore Size and Functionality in Isoreticular MOFs and Their Application in Methane Storage. *Science* **2002**, *295*, 469–472. [CrossRef]
78. Aljammal, N.; Jabbour, C.; Chaemchuen, S.; Juzsakova, T.; Verpoort, F. Flexibility in Metal–Organic Frameworks: A Basic Understanding. *Catalysts* **2019**, *9*, 512. [CrossRef]
79. Luo, Z.; Chaemchuen, S.; Zhou, K.; Verpoort, F. Ring-Opening Polymerization of L-Lactide to Cyclic Poly(Lactide) by Zeolitic Imidazole Framework ZIF-8 Catalyst. *ChemSusChem* **2017**, *10*, 4135–4139. [CrossRef]
80. Chughtai, A.H.; Ahmad, N.; Younus, H.A.; Laypkov, A.; Verpoort, F. Metal–Organic Frameworks: Versatile Heterogeneous Catalysts for Efficient Catalytic Organic Transformations. *Chem. Soc. Rev.* **2015**, *44*, 6804–6849. [CrossRef] [PubMed]
81. Yabushita, M.; Li, P.; Islamoglu, T.; Kobayashi, H.; Fukuoka, A.; Farha, O.K.; Katz, A. Selective Metal–Organic Framework Catalysis of Glucose to 5-Hydroxymethylfurfural Using Phosphate-Modified NU-1000. *Ind. Eng. Chem. Res.* **2017**, *56*, 7141–7148. [CrossRef]
82. Aljammal, N.; Lenssens, A.; Reviere, A.; Verberckmoes, A.; Thybaut, J.W.; Verpoort, F.; Heynderickx, P.M. Metal–Organic Frameworks as Catalysts for Fructose Conversion into 5-hydroxymethylfurfural: Catalyst Screening and Parametric Study. *Appl. Organomet. Chem.* **2021**, *35*, e6419. [CrossRef]
83. Wang, K.; Liu, Y.; Wu, W.; Chen, Y.; Fang, L.; Li, W.; Ji, H. Production of Levulinic Acid via Cellulose Conversion over Metal Oxide-Loaded MOF Catalysts in Aqueous Medium. *Catal. Lett.* **2020**, *150*, 322–331. [CrossRef]
84. Chen, J.; Li, K.; Chen, L.; Liu, R.; Huang, X.; Ye, D. Conversion of Fructose into 5-Hydroxymethylfurfural Catalyzed by Recyclable Sulfonic Acid-Functionalized Metal–Organic Frameworks. *Green Chem.* **2014**, *16*, 2490–2499. [CrossRef]
85. Akiyama, G.; Matsuda, R.; Sato, H.; Takata, M.; Kitagawa, S. Cellulose Hydrolysis by a New Porous Coordination Polymer Decorated with Sulfonic Acid Functional Groups. *Adv. Mater.* **2011**, *23*, 3294–3297. [CrossRef]
86. Liu, S.; Meng, Y.; Li, H.; Yang, S. Hierarchical Porous Mil-101(Cr) Solid Acid-Catalyzed Production of Value-Added Acetals from Biomass-Derived Furfural. *Polymers* **2021**, *13*, 3498. [CrossRef]
87. Chatterjee, A.; Hu, X.; Lam, F.L.-Y. A Dual Acidic Hydrothermally Stable MOF-Composite for Upgrading Xylose to Furfural. *Appl. Catal. A Gen.* **2018**, *566*, 130–139. [CrossRef]
88. Liu, X.F.; Li, H.; Zhang, H.; Pan, H.; Huang, S.; Yang, K.L.; Yang, S. Efficient Conversion of Furfuryl Alcohol to Ethyl Levulinate with Sulfonic Acid-Functionalized MIL-101(Cr). *RSC Adv.* **2016**, *6*, 90232–90238. [CrossRef]
89. Xu, S.; Pan, D.; Wu, Y.; Song, X.; Gao, L.; Li, W.; Das, L.; Xiao, G. Efficient Production of Furfural from Xylose and Wheat Straw by Bifunctional Chromium Phosphate Catalyst in Biphasic Systems. *Fuel Process. Technol.* **2018**, *175*, 90–96. [CrossRef]
90. Zhao, H.; Holladay, J.E.; Brown, H.; Zhang, Z.C. Metal Chlorides in Ionic Liquid Solvents Convert Sugars to 5-Hydroxymethylfurfural. *Science* **2007**, *316*, 1597–1600. [CrossRef]
91. Shao, Y.; Ding, Y.; Dai, J.; Long, Y.; Hu, Z.T. Synthesis of 5-Hydroxymethylfurfural from Dehydration of Biomass-Derived Glucose and Fructose Using Supported Metal Catalysts. *Green Synth. Catal.* **2021**, *2*, 187–197. [CrossRef]
92. Paul, G.; Iga, G.D.; Cabral, N.M.; Bueno, C.; Bisio, C.; Gallo, J.M.R. General Niobium Phosphates as Bifunctional Catalysts for the Conversion of Biomass-Derived Monosaccharides. *Appl. Catal. A* **2021**, *617*, 118099. [CrossRef]
93. Zhang, T.; Li, W.; Xin, H.; Jin, L.; Liu, Q. Production of HMF from Glucose Using an Al³⁺-Promoted Acidic Phenol-Formaldehyde Resin Catalyst. *Catal. Commun.* **2019**, *124*, 56–61. [CrossRef]

94. Palma, V.; Barba, D.; Cortese, M.; Martino, M.; Renda, S.; Meloni, E. Microwaves and Heterogeneous Catalysis: A Review on Selected Catalytic Processes. *Catalysts* **2020**, *10*, 246. [[CrossRef](#)]
95. Bromberg, L.; Su, X.; Hatton, T.A. Functional Networks of Organic and Coordination Polymers: Catalysis of Fructose Conversion. *Chem. Mater.* **2014**, *26*, 6257–6264. [[CrossRef](#)]
96. Guo, W.; Zhang, Z.; Hacking, J.; Heeres, H.J.; Yue, J. Selective Fructose Dehydration to 5-Hydroxymethylfurfural from a Fructose-Glucose Mixture over a Sulfuric Acid Catalyst in a Biphasic System: Experimental Study and Kinetic Modelling. *Chem. Eng. J.* **2021**, *409*, 128182. [[CrossRef](#)]
97. Testa, M.L.; Miroddi, G.; Russo, M.; La Parola, V.; Marci, G. Dehydration of Fructose to 5-HMF over Acidic TiO₂ Catalysts. *Materials* **2020**, *13*, 1178. [[CrossRef](#)] [[PubMed](#)]
98. Carraher, J.M.; Fleitman, C.N.; Tessonier, J.P. Kinetic and Mechanistic Study of Glucose Isomerization Using Homogeneous Organic Brønsted Base Catalysts in Water. *ACS Catal.* **2015**, *5*, 3162–3173. [[CrossRef](#)]
99. Li, X.; Wang, Y.; Xie, X.; Huang, C.; Yang, S. Dehydration of Fructose, Sucrose and Inulin to 5-Hydroxymethylfurfural over Yeast-Derived Carbonaceous Microspheres at Low Temperatures. *RSC Adv.* **2019**, *9*, 9041–9048. [[CrossRef](#)]
100. Van Putten, R.J.; Van Der Waal, J.C.; De Jong, E.; Rasrendra, C.B.; Heeres, H.J.; De Vries, J.G. Hydroxymethylfurfural, a Versatile Platform Chemical Made from Renewable Resources. *Chem. Rev.* **2013**, *113*, 1499–1597. [[CrossRef](#)] [[PubMed](#)]
101. Ji, T.; Li, Z.; Liu, C.; Lu, X.; Li, L.; Zhu, J. Niobium-Doped TiO₂ Solid Acid Catalysts: Strengthened Interfacial Polarization, Amplified Microwave Heating and Enhanced Energy Efficiency of Hydroxymethylfurfural Production. *Appl. Catal. B Environ.* **2019**, *243*, 741–749. [[CrossRef](#)]
102. Zhang, A.; Li, M.; Wang, D.; Li, Y.; Zhang, Q.; Kong, J. Enhanced Electromagnetic Wave Absorption of Polar Absorber Hybrids Self-Assembled by MWCNTs and Sulfonated Polystyrene Microsphere. *J. Mater. Sci.* **2020**, *55*, 1637–1647. [[CrossRef](#)]
103. Li, C.; Zhang, Y.; Ji, S.; Jiang, X.; Zhang, Z.; Yu, L. Microwave Absorption Properties of γ -Fe₂O₃/(SiO₂)_x-SO₃H/Polypyrrole Core/Shell/Shell Microspheres. *J. Mater. Sci.* **2018**, *53*, 5270–5286. [[CrossRef](#)]
104. Nüchter, M.; Ondruschka, B.; Jungnickel, A.; Müller, U. Organic Processes Initiated by Non-Classical Energy Sources. *J. Phys. Org. Chem.* **2000**, *13*, 579–586. [[CrossRef](#)]
105. Asakuma, Y.; Ogawa, Y.; Maeda, K.; Fukui, K.; Kuramochi, H. Effects of Microwave Irradiation on Triglyceride Transesterification: Experimental and Theoretical Studies. *Biochem. Eng. J.* **2011**, *58–59*, 20–24. [[CrossRef](#)]
106. Wang, L.; Zhang, L.; Li, H.; Ma, Y.; Zhang, R. High Selective Production of 5-Hydroxymethylfurfural from Fructose by Sulfonic Acid Functionalized SBA-15 Catalyst. *Compos. Part B Eng.* **2019**, *156*, 88–94. [[CrossRef](#)]
107. Ji, T.; Tu, R.; Li, L.; Mu, L.; Liu, C.; Lu, X.; Zhu, J. Environmental Localizing Microwave Heat by Surface Polarization of Titanate Nanostructures for Enhanced Catalytic Reaction Efficiency. *Appl. Catal. B Environ.* **2018**, *227*, 266–275. [[CrossRef](#)]
108. Qi, X.; Watanabe, M.; Aida, T.M.; Smith, R.L. Catalytic Dehydration of Fructose into 5-Hydroxymethylfurfural by Ion-Exchange Resin in Mixed-Aqueous System by Microwave Heating. *Green Chem.* **2008**, *10*, 799–805. [[CrossRef](#)]
109. Lee, Y.; Lee, C.; Yoon, J. Kinetics and Mechanisms of DMSO (Dimethylsulfoxide) Degradation by UV/H₂O₂ Process. *Water Res.* **2004**, *38*, 2579–2588. [[CrossRef](#)]
110. Tudino, T.C.; Nunes, R.S.; Mandelli, D.; Carvalho, W.A. Influence of Dimethylsulfoxide and Dioxygen in the Fructose Conversion to 5-Hydroxymethylfurfural Mediated by Glycerol's Acidic Carbon. *Front. Chem.* **2020**, *8*, 263. [[CrossRef](#)] [[PubMed](#)]
111. Whitaker, M.R.; Parulkar, A.; Ranadive, P.; Joshi, R.; Brunelli, N.A. Examining Acid Formation during the Selective Dehydration of Fructose to 5-hydroxymethylfurfural in Dimethyl Sulfoxide and Water. *ChemSusChem* **2019**, *12*, 2211–2219. [[CrossRef](#)]
112. Hu, X.; Lievens, C.; Larcher, A.; Li, C.Z. Reaction Pathways of Glucose during Esterification: Effects of Reaction Parameters on the Formation of Humins Type Polymers. *Bioresour. Technol.* **2011**, *102*, 10104–10113. [[CrossRef](#)]
113. Van de Steene, E.; De Clercq, J.; Thybaut, J.W. Ion-Exchange Resin Catalyzed Transesterification of Ethyl Acetate with Methanol: Gel versus Macroporous Resins. *Chem. Eng. J.* **2014**, *242*, 170–179. [[CrossRef](#)]
114. Antonetti, C.; Fulignati, S.; Licursi, D.; Maria, A.; Galletti, R. Turning Point towards the Sustainable Production of HMF in Water: Metal Salts for Its Synthesis from Fructose and Inulin. *ACS Sustain. Chem. Eng.* **2019**, *7*, 6830–6838. [[CrossRef](#)]
115. Esmaeili, N.; Zohuriaan-Mehr, M.J.; Bouhendi, H.; Bagheri-Marandi, G. HMF Synthesis in Aqueous and Organic Media under Ultrasonication, Microwave Irradiation and Conventional Heating. *Korean J. Chem. Eng.* **2016**, *33*, 1964–1970. [[CrossRef](#)]
116. Kunov-kruse, A.J.; Riisager, A.; Saravanamurugan, S.; Berg, R.W.; Fehrmann, R. Revisiting the Brønsted Acid Catalysed Hydrolysis Kinetics of Polymeric Carbohydrates in Ionic Liquids by in Situ ATR-FTIR Spectroscopy. *Green Chem.* **2013**, *15*, 2843–2848. [[CrossRef](#)]
117. Yang, F.; Tong, X.; Xia, F.; Zheng, C.; Qin, L.; Jiang, X. Efficient Hydroxymethylfurfural Production over Phosphoric Carbon Solid Acids. *Catal. Lett.* **2018**, *148*, 1848–1855. [[CrossRef](#)]
118. Ferrari, A.; Hunt, J.; Lita, A.; Ashley, B.; Stiegman, A.E. Microwave-Specific Effects on the Equilibrium Constants and Thermodynamics of the Steam-carbon and Related Reactions. *J. Phys. Chem. C* **2014**, *118*, 9346–9356. [[CrossRef](#)]
119. Priece, P.; Lopez-Sanchez, J.A. Advantages and Limitations of Microwave Reactors: From Chemical Synthesis to the Catalytic Valorization of Biobased Chemicals. *ACS Sustain. Chem. Eng.* **2019**, *7*, 3–21. [[CrossRef](#)]
120. Nayak, S.N.; Nayak, M.G.; Bhasin, D.C.P. Parametric, Kinetic, and Thermodynamic Studies of Microwave-Assisted Esterification of Kusum Oil. *Fuel Commun.* **2021**, *8*, 100018. [[CrossRef](#)]
121. Perreux, L.; Loupy, A. A Tentative Rationalization of Microwave Effects in Organic Synthesis According to the Reaction Medium, and Mechanistic Considerations. *Tetrahedron* **2001**, *57*, 9199–9223. [[CrossRef](#)]

122. Saha, B.; Abu-Omar, M.M. Advances in 5-Hydroxymethylfurfural Production from Biomass in Biphasic Solvents. *Green Chem.* **2013**, *16*, 24–38. [[CrossRef](#)]
123. Qi, X.; Watanabe, M.; Aida, T.M.; Smith, R.L. Selective Conversion of D-Fructose to 5-Hydroxymethylfurfural by Ion-Exchange Resin in Acetone/Dimethyl Sulfoxide Solvent Mixtures. *Ind. Eng. Chem. Res.* **2008**, *30*, 9234–9239. [[CrossRef](#)]
124. Moreau, C.; Durand, R.; Razigade, S.; Duhamet, J.; Faugeras, P.; Rivalier, P.; Pierre, R.; Avignon, G. Dehydration of Fructose to 5-Hydroxymethylfurfural over H-Mordenites. *Appl. Catal. A Gen.* **1996**, *145*, 211–224. [[CrossRef](#)]
125. Villanueva, N.I.; Marzialetti, T.G. Mechanism and Kinetic Parameters of Glucose and Fructose Dehydration to 5-Hydroxymethylfurfural over Solid Phosphate Catalysts in Water. *Catal. Today* **2018**, *302*, 100–107. [[CrossRef](#)]
126. Floris, B.; Sabuzi, F.; Galloni, P.; Conte, V. The Beneficial Sinergy of MW Irradiation and Ionic Liquids in Catalysis of Organic Reactions. *Catalysts* **2017**, *7*, 261. [[CrossRef](#)]
127. Qi, X.; Watanabe, M.; Aida, T.M.; Smith, R.L. Efficient Process for Conversion of Fructose to 5-Hydroxymethylfurfural with Ionic Liquids. *Green Chem.* **2009**, *11*, 1327–1331. [[CrossRef](#)]
128. Nunes, R.S.; Reis, G.M.; Vieira, L.M.; Mandelli, D.; Carvalho, W.A. Ultra-Fast Selective Fructose Dehydration Promoted by a Kraft Lignin Sulfonated Carbon Under Microwave Heating. *Catal. Lett.* **2021**, *151*, 398–408. [[CrossRef](#)]
129. Qin, J.S.; Yuan, S.; Lollar, C.; Pang, J.; Alsalme, A.; Zhou, H.C. Stable Metal-Organic Frameworks as a Host Platform for Catalysis and Biomimetics. *Chem. Commun.* **2018**, *54*, 4231–4249. [[CrossRef](#)]
130. CEM. CEM Operation Manual. In *CEM Corporation Operation Manual*; CEM: Charlotte, NC, USA, 2006.
131. Kittrell, J.R. Mathematical Modeling of Chemical Reactions. In *Advances in Chemical Engineering*; Elsevier: Amsterdam, The Netherlands, 1970; Volume 8, pp. 97–183.
132. Stewart, W.E.; Caracotsios, M. Computer-Aided Modelling of Reactive Systems. In *Computer-Aided Modelling of Reactive Systems*; John Wiley & Sons: Hoboken, NJ, USA, 2008; p. 141, ISBN 9780470274958.

Disclaimer/Publisher's Note: The statements, opinions and data contained in all publications are solely those of the individual author(s) and contributor(s) and not of MDPI and/or the editor(s). MDPI and/or the editor(s) disclaim responsibility for any injury to people or property resulting from any ideas, methods, instructions or products referred to in the content.